NBS
PUBLICATIONS

NBSIR 81-1653

NAT'L INST. OF STAND & TECH
A11106 978984

# MODELLING OF OIL SHALE RETORTS FOR ELECTROMAGNETIC SENSING TECHNIQUES

H. Chew

Electromagnetic Fields Division
National Engineering Laboratory
National Bureau of Standards
Boulder, Colorado 80303

Prepared for:

U.S. Department of Energy
Laramie Energy Technology Center
Laramie, Wyoming 82071

November 1981

QC
100
.U56
81-1653
1981
c. 2

NATIONAL BUREAU
OF STANDARDS
LIBRARY
JAN 25 1982
Not Circ.
QC100
.U56
NO. 81-1653
1981
C.2

NBSIR 81-1653

# MODELLING OF OIL SHALE RETORTS FOR ELECTROMAGNETIC SENSING TECHNIQUES

H. Chew

Electromagnetic Fields Division
National Engineering Laboratory
National Bureau of Standards
Boulder, Colorado 80303

November 1981

Prepared for:

U.S. Department of Energy
Laramie Energy Technology Center
Laramie, Wyoming 82071

U.S. DEPARTMENT OF COMMERCE, Malcolm Baldrige, Secretary

NATIONAL BUREAU OF STANDARDS, Ernest Ambler, Director

CONTENTS

Page

I. INTRODUCTION.....1

II. FORMULATION OF THE PROBLEM.....5

III. NUMERICAL RESULTS AND DISCUSSION.....9

IV. CONCLUSIONS AND RECOMMENDATIONS.....18

ACKNOWLEDGMENTS.....20

REFERENCES.....21

APPENDIX 1.....22

APPENDIX 2.....24

APPENDIX 3 Listing of the Program.....27

LIST OF FIGURES

Figure 1. Schematic drawing of an oil shale retort.....2

Figure 2. A spheroidal retort. The major axis of the prolate spheroid is along the vertical z-axis. The transmitter lies in the x-z plane with spherical coordinates $(r_d, \theta_d, 0)$ and the receiver coordinates are $(r_o, \theta_o, \phi_o)$. The complex dielectric constants inside and outside are denoted by $\varepsilon$ and $\varepsilon_2$, respectively.....6

Figure 3. The geometry used in the computations: a = 45.7 m (150 ft), b = 25.1 m (82.5 ft), $r_d$ = 1.1 a, $\theta_d$ = 90°; $r_o$ = 1.05 a, $\theta_o$ = 0° (10°) 360°, f = 4 MHz, $k_o a = 2\pi a/\lambda$ = 3.84.....10

Figure 4. $|E_\theta|^2$ vs scattering angle; dipole along x-axis.....11

Figure 5. $|E_r|^2$ vs scattering angle; dipole along x-axis.....12

Figure 6. $|\vec{E}_{tot}|^2$ vs scattering angle; dipole along x-axis.....13

Figure 7. $|E_\phi|^2$ vs scattering angle; dipole along y-axis.....14

Figure 8. $|E_\theta|^2$ vs scattering angle; dipole along z-axis.....15

Figure 9. $|E_r|^2$ vs scattering angle; dipole along z-axis.....16

Figure 10. $|\vec{E}_{tot}|^2$ vs scattering angle; dipole along z-axis.....17

# MODELLING OF OIL SHALE RETORTS FOR ELECTROMAGNETIC SENSING TECHNIQUES

H. Chew*

We report here some work on the modelling of oil shale retorts for electromagnetic sensing techniques. The aim is to obtain useful information about the contents of the retort (e.g., rubble size, void ratio, etc.) by means of electromagnetic probes. In this work, the retort is modelled by a spheroid with an average dielectric constant which depends on the void ratio. The near field due to a radiating dipole source in the vicinity of a spheroidal retort is computed using the Extended Boundary Condition Method due to Waterman, Barber, and Yeh. Numerical results are given at 4 MHz for a retort with major axis 45.7 m (150 ft), minor axis 25.1 m (82.5 ft), bulk dielectric constant 8.8 + 3.7j, and various void ratios. The results indicate feasibility of determining the void ratio by remote electromagnetic measurements. It is also believed that this work may be of interest beyond the immediate context of oil shale retort modelling.

Key words: oil shale retorts; remote sensing; scattering.

## I. INTRODUCTION

In situ processing of oil shale offers many environmental advantages. For example, the waste products largely remain underground and are not released into the immediate environment. There are also many technical problems connected with in situ processing, one of them being the gathering of information about the contents and the state of the oil shale retorts. A promising method for obtaining such information is electromagnetic remote sensing. In this approach, transmitters and receivers are introduced to the vicinity of the retort via boreholes (figure 1), and one attempts to extract information about the contents of the retort by analyzing the received signals. For this purpose, it is necessary to have a specific model which relates the relevant physical quantities and allows the interpretation of the signals.

The precise modelling of a retort of irregular shape containing rubble of irregular size and shape is a difficult task both in principle and numerically. To obtain tractable results, many simplifying assumptions are unavoidable. In this work, we model the retort by a spheroid embedded in an infinite medium of different electromagnetic properties (there is no

*On sabbatical leave (1980-1981) from Department of Physics, Clarkson College, Potsdam, NY 13676.

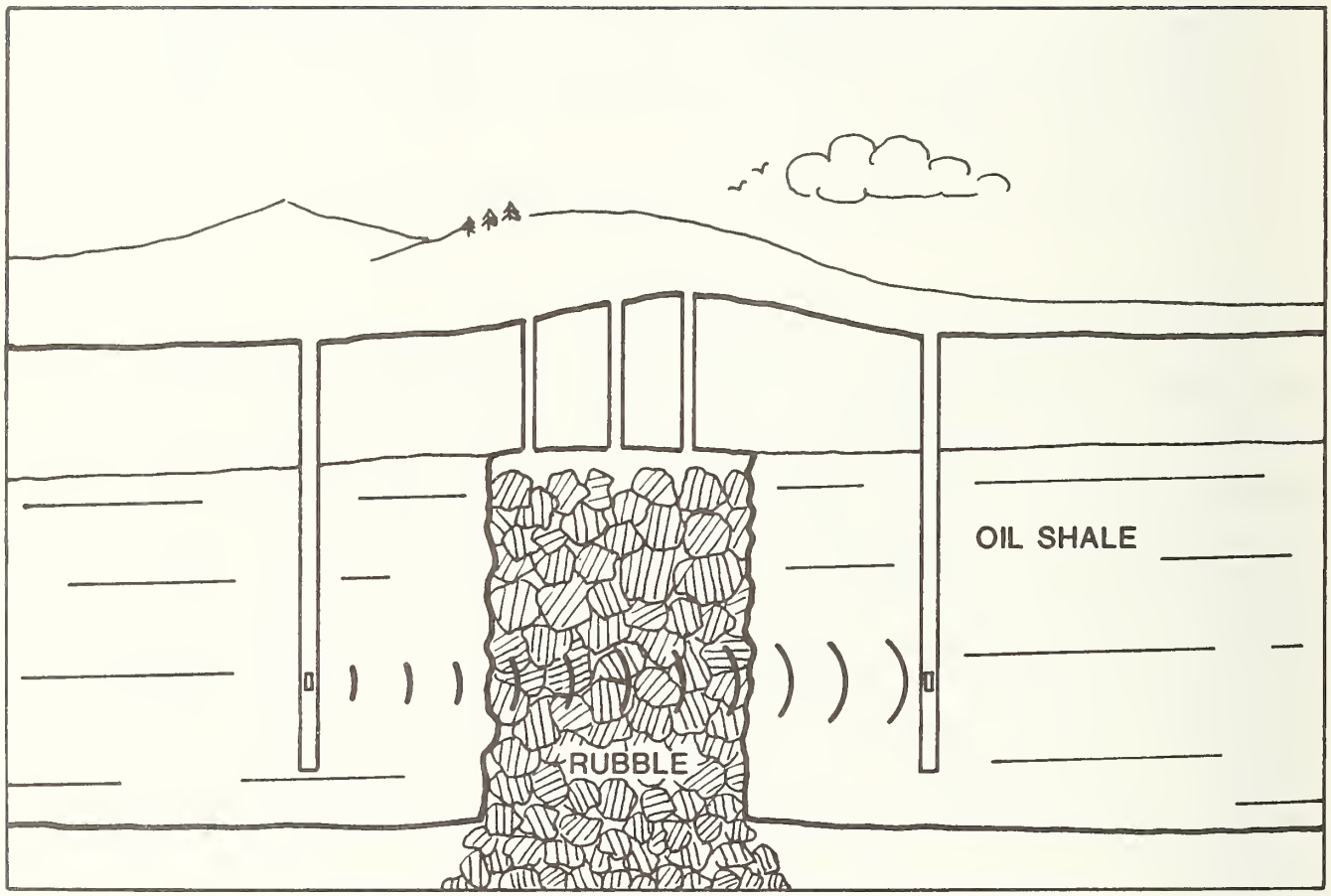


Figure 1. Schematic drawing of an oil shale retort.

difficulty in treating media of different magnetic permeabilities, although in the numerical work to be presented here both media are assumed to be non-magnetic), and compute the near field due to a radiating dipole source in the vicinity of the retort using the Extended Boundary Condition Method (EBCM) of Waterman [1], Barber and Yeh [2]. The effects of the boreholes are neglected, and both the spheroid and the outside medium are assumed to be homogeneous and isotropic. In practice, the shale rocks generally have some layered structure, but the effects of anisotropy are probably not large, as laboratory measurements at the National Bureau of Standards [3] show that the value of the dielectric constant of shale rocks is essentially independent of orientation. With these assumptions, the EBCM formalism is exact in the sense that the resulting series is a solution to Maxwell's equations satisfying the appropriate boundary conditions and therefore contains all the electromagnetic effects (surface waves, body waves, etc.). Moreoever, the spheroid, with its two geometric parameters (the major and minor axes) is sufficiently flexible to simulate a variety of shapes and yet is such that the mathematical analysis involved is manageable, if complicated. A drawback of this approach is the complexity of the calculations, which are time consuming even when done on a fast electronic computer. The near field calculated, which includes both the incident dipole field and the scattered field in the near zone, is a function of the characteristics of the retort and of the surrounding medium. The mixture of rubble and void inside the retort is described here by an average dielectric constant which depends, among other things, on the void ratio (defined as the ratio of the void volume to the total retort volume) in a way to be discussed later. Thus, the dependence of the field on the average dielectric constant may be used to extract information about the contents of the retort. In this work, we are able to treat only the question of void ratio and not that of rubble size. To gain some idea of this dependence without elaborate formulas, we carried out a preliminary calculation (Appendix 1) for a spherical retort in the Rayleigh limit, and found that the scattered field is a sensitive function of the average dielectric constant inside, being roughly proportional to the difference between the dielectric constants inside and outside. This strong dependence appears to persist in the much more involved spheroidal calculations as well.

The relation between the average dielectric constant and the void content is a difficult subject, and a large number of workers [4,5,6] have examined

the problem of the effective dielectric constant of two-component systems. For example, Sillars [7] obtained an expression for the dielectric constant of a two-component system in terms of those of the constituents and the volume ratios for the case when one component consists of spheroids of uniform size embedded in the other medium. His result also depends on the ratio of the spheroidal axes. Because the rubble is very unlikely to be spheroids of uniform size, it is uncertain whether his result would be applicable to our case, inasumch as it introduces an additional parameter (the ratio of the axes). More complicated and frequency-dependent results are also available [5], again under assumptions of doubtful applicability to oil shale retorts. In this work, we shall use a simple empirical relation due to Lichtenecker [6], wherein the logarithm of the dielectric constant is averaged in proportion to the volume. If two media of dielectric constants $\varepsilon_1$ and $\varepsilon_2$ and volumes $V_1$ and $V_2$, respectively, form a composite medium whose average dielectric constant is $\varepsilon$ (throughout this paper, dielectric constants refer to dielectric constants relative to that of vacuum, except in eq (3)), then it has been found empirically that in a large number of cases [6,8], $\varepsilon$ is given to a good approximation by

$$\ln \varepsilon = \frac{V_1}{V} \ln \varepsilon_1 + \frac{V_2}{V} \ln \varepsilon_2 , \tag{1}$$

where $V = V_1 + V_2$ is the total volume. In the case of an oil shale retort, which consists of air (dielectric constant $\varepsilon_1 = 1$) and rubble (dielectric constant $\varepsilon_2$ = bulk value for shale rocks), the void ratio is $V_1/V$ and we may rewrite (1) as

$$\ln \varepsilon = \frac{V - V_1}{V} \ln \varepsilon_2 = (1 - V_1/V) \ln \varepsilon_2 . \tag{1a}$$

This relation, which will be referred to as Lichtenecker's formula, will be used to relate the void ratio $V_1/V$ to the average dielectric constant of the interior of the retort (rubble plus void), with the bulk dielectric constant $\varepsilon_2$ of the exterior medium being assumed known. In the case of absorbing media, eq (1a) is assumed to hold for both the real and imaginary parts of the dielectric constant. This relation neglects the dependence of the average dielectric constant on the size and shape of the rubble. This neglect may not be very serious [6], as there is some evidence from the recent work of Warne and Uhl [5], who concluded from some one-dimensional computer simulation calculations that scattering effects depend largely on void dimensions rather than rock sizes.

## II. FORMULATION OF THE PROBLEM

In applying the Extended Boundary Condition Method [1,2], the scatterer is replaced by a set of equivalent surface currents. The incident and scattered fields are both expanded in series of vector spherical harmonics. After a lengthy analysis [1,2], a transition matrix (T-matrix) is computed which converts the known coefficients of the incident field into the scattering coefficients. The elements of the T-matrix are surface integrals of certain combinations of Bessel and Legendre functions which are computed numerically. For the convenience of the reader, we summarize the key steps involved.

Let the spheroid be centered at the origin with its axis of symmetry (z-axis) vertical (figure 2), and the oscillating dipole source with dipole moment $\vec{P}$ be located at coordinate $\vec{r}_d$. If the observer is at the coordinate $\vec{r}_o = \vec{r}$, then for $r>r_d$ the incident dipole field may be expanded in a series of vector spherical harmonics (if $r<r_d$ one needs only to interchange the superscripts 1 and 3 in eqs (2) and (3)),

$$\vec{E}_i(\vec{r}) = \sum_V D_v \left[a_v \vec{M}^3_v(k_2\vec{r}) + b_v \vec{N}^3_v(k_2\vec{r})\right], \tag{2}$$

where $k_2$ = wave number in medium 2

$$D_v = \varepsilon_m \frac{(2n+1)(n-m)!}{4n(n+1)(n+m)!}, \quad \varepsilon_m = \begin{cases} 1 & (m=0) \\ 2 & (m>0) \end{cases}$$

$$\sum_V = \sum_{e,o} \sum_{n=1}^{\infty} \sum_{m=0}^{m=n}$$

$$a_v = \frac{jk_2^3}{\pi\varepsilon_2} \vec{p} \cdot \vec{M}^1_v(k_2\vec{r}_d), \quad b_v = \frac{jk_2^3}{\pi\varepsilon_2} \vec{p} \cdot \vec{N}^1_v(k_2\vec{r}_d). \tag{3}$$

The label v stands for three indices: m=0,1,•••n; n=1,2,3•••; σ=odd, even. Explicitly, we have

$$\vec{M}^1_{\sigma mn}(k_2\vec{r}) = \nabla\times\left[\vec{r} \begin{matrix}\cos m\phi \\ \sin m\phi\end{matrix} P^m_n(\cos\theta)\, j_n(k_2 r)\right], \tag{4a}$$

$$\vec{M}^3_{\sigma mn}(k_2\vec{r}) = \vec{M}^1_{\sigma mn}(k_2\vec{r}) \text{ with } j_n(k_2r) \text{ replaced by } h^{(1)}_n(k_2r), \tag{4b}$$

$$\vec{N}^\alpha_{\sigma mn}(k_2\vec{r}) = \frac{1}{k_2}\nabla\times\vec{M}^\alpha_{\sigma mn}(k_2\vec{r}), \quad \alpha = 1,3. \tag{4c}$$

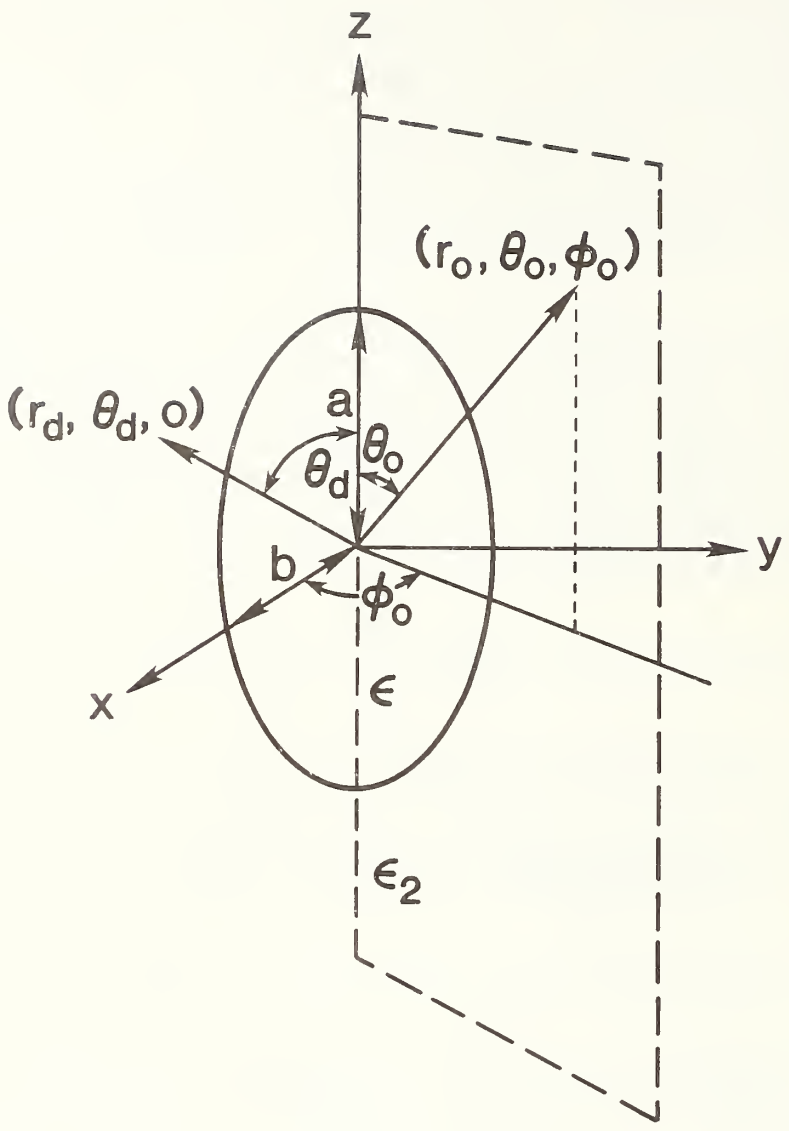


Figure 2. A spheroidal retort. The major axis of the prolate spheroid is along the vertical z-axis. The transmitter lies in the x-z plane with spherical coordinates $(r_d, \theta_d, 0)$ and the receiver cordinates are $(r_o, \theta_o, \phi_o)$. The complex dielectric constants inside and outside are denoted by $\varepsilon$ and $\varepsilon_2$, respectively.

For a scatterer of finite conductivity, the EBCM requires as an intermediate step also the field inside the scatterer. Let this field be $\vec{E}(\vec{r})$, with the expansions (k = wave number inside the scatterer),

$$\vec{E}(\vec{r}) = \sum_{v} [c_v \vec{M}^1_v (k\vec{r}) + d_v \vec{N}^1_v (k\vec{r})], \tag{5}$$

and

$$\vec{E}_{sc}(\vec{r}) = \sum_{v} [p_v \vec{M}^3_v (k_2\vec{r}) + q_v \vec{N}^3_v (k_2\vec{r})]. \tag{6}$$

Then the internal field coefficients $c_v$ and $d_v$ may be found from the linear equations

$$\sum_{v} \{ [K_{\mu v} + \sqrt{\frac{\varepsilon_r}{\mu_r}}\, J_{\mu v}] c_v + [L_{\mu v} + \sqrt{\frac{\varepsilon_r}{\mu_r}}\, I_{\mu v}] dv \} = - j\, a_\mu \tag{7a}$$

$$\sum_{v} \{ [I_{\mu v} + \sqrt{\frac{\varepsilon_r}{\mu_r}}\, L_{\mu v}] c_v + [J_{\mu v} + \sqrt{\frac{\varepsilon_r}{\mu_r}}\, K_{\mu v}] d_v \} = - j\, b_\mu , \tag{7b}$$

where $\varepsilon_r = \varepsilon/\varepsilon_2$, $\mu_r = \mu/\mu_2$, and

$$I_{\mu v} = \frac{k_2^2}{\pi} \int \hat{n} \cdot [\vec{M}^3_\mu (k_2\vec{r}') \times \vec{M}^1_v (k\vec{r}')]\, dS, \tag{8a}$$

$$J_{\mu v} = \frac{k_2^2}{\pi} \int \hat{n} \cdot [\vec{M}^3_\mu (k_2\vec{r}') \times \vec{N}^1_v (k\vec{r}')]\, dS, \tag{8b}$$

$$K_{\mu v} = \frac{k_2^2}{\pi} \int \hat{n} \cdot [\vec{N}^3_\mu (k_2\vec{r}') \times \vec{M}^1_v (k\vec{r}')]\, dS, \tag{8c}$$

$$L_{\mu v} = \frac{k_2^2}{\pi} \int \hat{n} \cdot [\vec{N}^3_\mu (k_2\vec{r}') \times \vec{N}^1_v (k\vec{r}')]\, dS. \tag{8d}$$

The integrations are over the surface S of the spheroid (area element dS and unit outward normal $\hat{n}$ ). After the internal field coefficients $c_\mu$ and $d_\mu$ are determined in terms of the known incident coefficients $a_\mu$ and $b_\mu$, the required scattering coefficients $p_\mu$ and $q_\mu$ are given by

$$p_\mu = -j D_\mu \sum_\nu \{[K'_{\mu\nu} + \sqrt{\frac{\varepsilon_r}{\mu_r}}\, J'_{\mu\nu}]\, c_\nu + [L'_{\mu\nu} + \sqrt{\frac{\varepsilon_r}{\mu_r}}\, I'_{\mu\nu}]\, d_\nu\} \quad (9a)$$

$$q_\mu = -j D_\mu \sum_\nu \{[I'_{\mu\nu} + \sqrt{\frac{\varepsilon_r}{\mu_r}}\, L'_{\mu\nu}]\, c_\nu + [J'_{\mu\nu} + \sqrt{\frac{\varepsilon_r}{\mu_r}}\, K'_{\mu\nu}]\, d_\nu\}\ , \quad (9b)$$

where $I'_{\mu\nu}$, $J'_{\mu\nu}$, $K'_{\mu\nu}$ and $L'_{\mu\nu}$ are obtained from the corresponding unprimed quantities by replacing the upper index 3 in the first vector spherical harmonics in the surface integrals by the index 1.

The total field at the observer coordinate $\vec{r}_o = \vec{r}$ is the sum of the incident field $\vec{E}_i(\vec{r})$ and the scattered field $\vec{E}_{sc}(\vec{r})$. Because the receiver is not in general in the far zone, the total field must be calculated with the exact $\vec{M}^3$ and $\vec{N}^3$'s rather than the asymptotic forms used in most scattering calculations. In the near zone, the radial component of the field is in general comparable to the $\theta$- and $\phi$-components. While the total field can be calculated from the series expansion in principle, it proved virtually impossible to obtain convergence in general when the incident dipole field was included. The reason is that the terms in the dipole field expansion (see eqs (3) and (4)) contains products of spherical Bessel and Neumann functions which are usually such that when one factor becomes small, the other becomes large, so that the product stays almost constant even when a large number of terms are used. Accordingly, a separate subroutine was written to calculate the dipole term separately from the closed-form expression [12], and the result was added to the scattered field after the convergence of the latter was ascertained.

In the calculation of the scattered field, it is necessary to check convergence with respect to three quantities: the number of m values, the number of n values (NRANK), and the number of sections (NDPS) in the numerical integration. Because the number of m values does not exceed n + 1, the first check is straightforward. Convergence with respect to the last two quantities can be ascertained only by the slow process of increasing each until the results converge at all angles. For 4 MHz and the physical parameters used here, convergence was obtained for $N_m \sim 12$, NRANK ~ 32, and NDPS $\leqslant$ 100. All these will go up if either the frequency or the dielectric constants are increased.

## III. NUMERICAL RESULTS AND DISCUSSION

In figures 4-10, we show the magnitude squares of the spherical components of the total (dipole plus scattered) electric field and their sum at the receiver (observer) coordinate $(r_o, \theta_o, \phi_o)$, where $\phi_o = 0$. The coordinate system is chosen so that the origin is at the center of the spheroid and the z-axis along the symmetry axis. The dipole transmitter lies in the x-z plane so that its spherical coordinates are $(r_d, \theta_d, 0)$. This choice of the x-z plane, which involves no loss of generality, simplifies the incident field coefficients greately, because with $\phi_d = 0$, all the terms with the factor sin $m\phi_d$ (see eqs (3) and (4)) are now zero while cos m $\phi_d$ becomes unity independent of m. The curves have been plotted for $r_o$ = 1.05 a, or 1.05 times the major axis, and $r_d$ = 1.1 a, $\theta_d = 90°$, while $\theta_o$ runs in steps of 10° from 0° to 360°. Results are shown for unit dipole strength and three orthogonal dipole orientations: $\vec{p}$ along the x, y, z axes, respectively. For all these orientations (but of course not in general), the curves are symmetric with respect to the x-axis ($\theta_o = 90°$ and $\theta_o = 270°$), so only the angular interval $90^0 < \theta_o \leq 270^0$ is shown. Note that at $\theta_o = 90°$, both the transmitter and receiver are on the positive x-axis at a short distance 0.05 a apart, so the fields are very large in general. Because of the way the coordinate axes are chosen, the electric field at the receiver has only $\theta$- and r-components when the dipole source oscillates along the x- or z-axis, and only a $\phi$-component when the dipole oscillates along the y-axis. In the last case, $|E_{tot}|^2$ is simply equal to $|E_\phi|^2$.

The other physical parameters are shown in figure 3. The axes a and b are taken to be the vertical and horizontal dimensions of an operating Occidental Petroleum oil shale retort at Logan Wash, Colorado. In figures 4-10, each figure shows four curves corresponding to void ratios 10%, 15%, 20%, and 25%, respectively. The corresponding values of the average dielectric constant $\varepsilon$ are calculated with the Lichtenecker formula from the bulk value [3] 8.8 + 3.7 j : 7.08 + 3.25 j (10% void), 6.35 + 3.0 j (15% void), 5.70 + 2.85 j (20% void), and 5.11 + 2.67 j (25% void).

It will be seen that the curves have generally more structure for $\theta_o < 180°$ (the transmitter side) than for $\theta_o > 180°$ (the far side). Much of this structure arises from the complex interference between the scattered field and the incident dipole field. Because the outside medium is highly lossy (Im $\varepsilon_2$ = 3.7), the dipole field is much attenuated on the far side, so the field

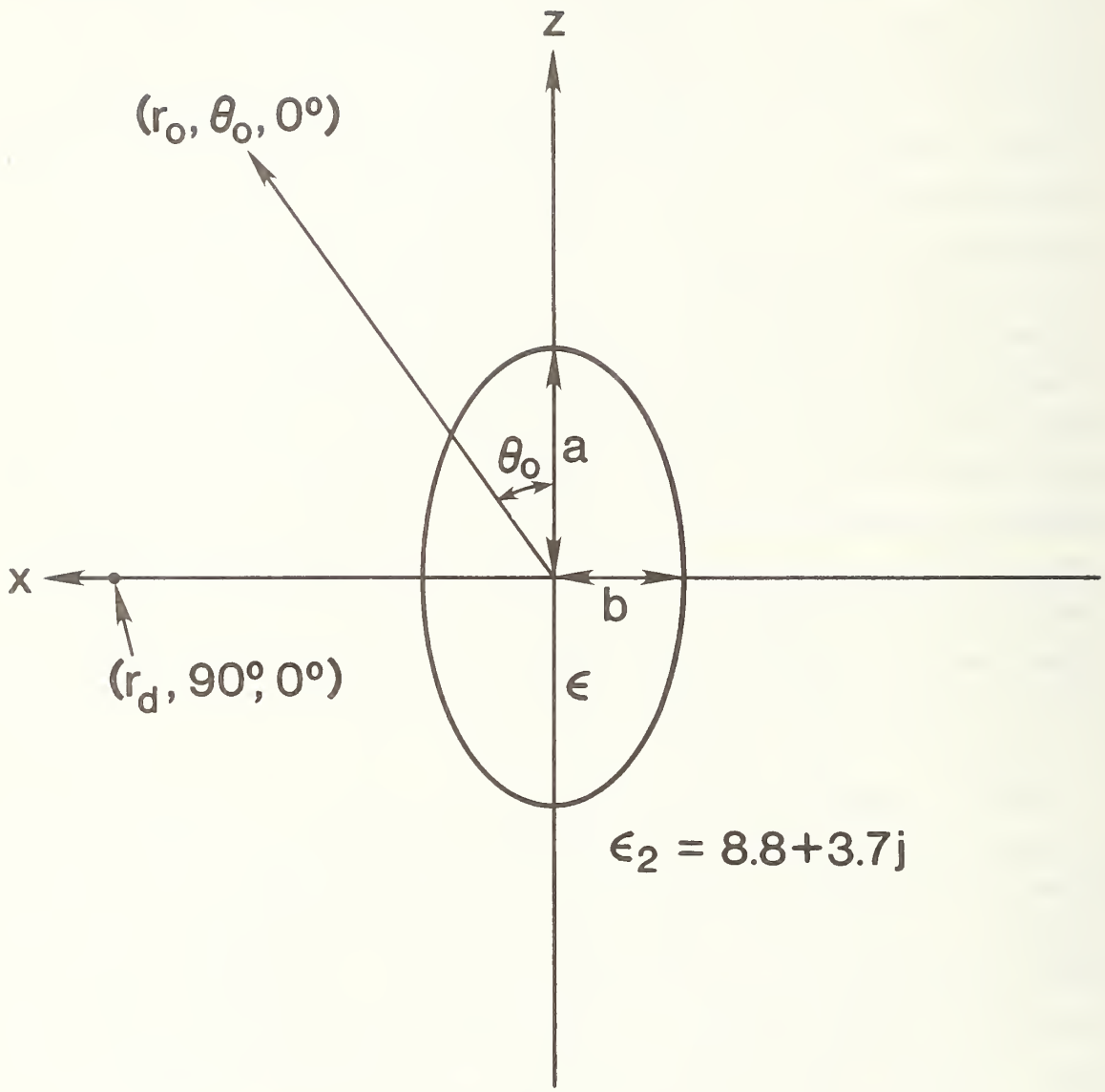


Figure 3. The geometry used in the computations: a = 45.7 m (150 ft), b = 25.1 m (82.5 ft), $r_d$ = 1.1 a, $\theta_d$ = 90°, $r_o$ = 1.05 a, $\theta_o$ = 0° (10°) 360°, f = 4 MHz, $k_o a = 2\pi a/\lambda$ = 3.84.

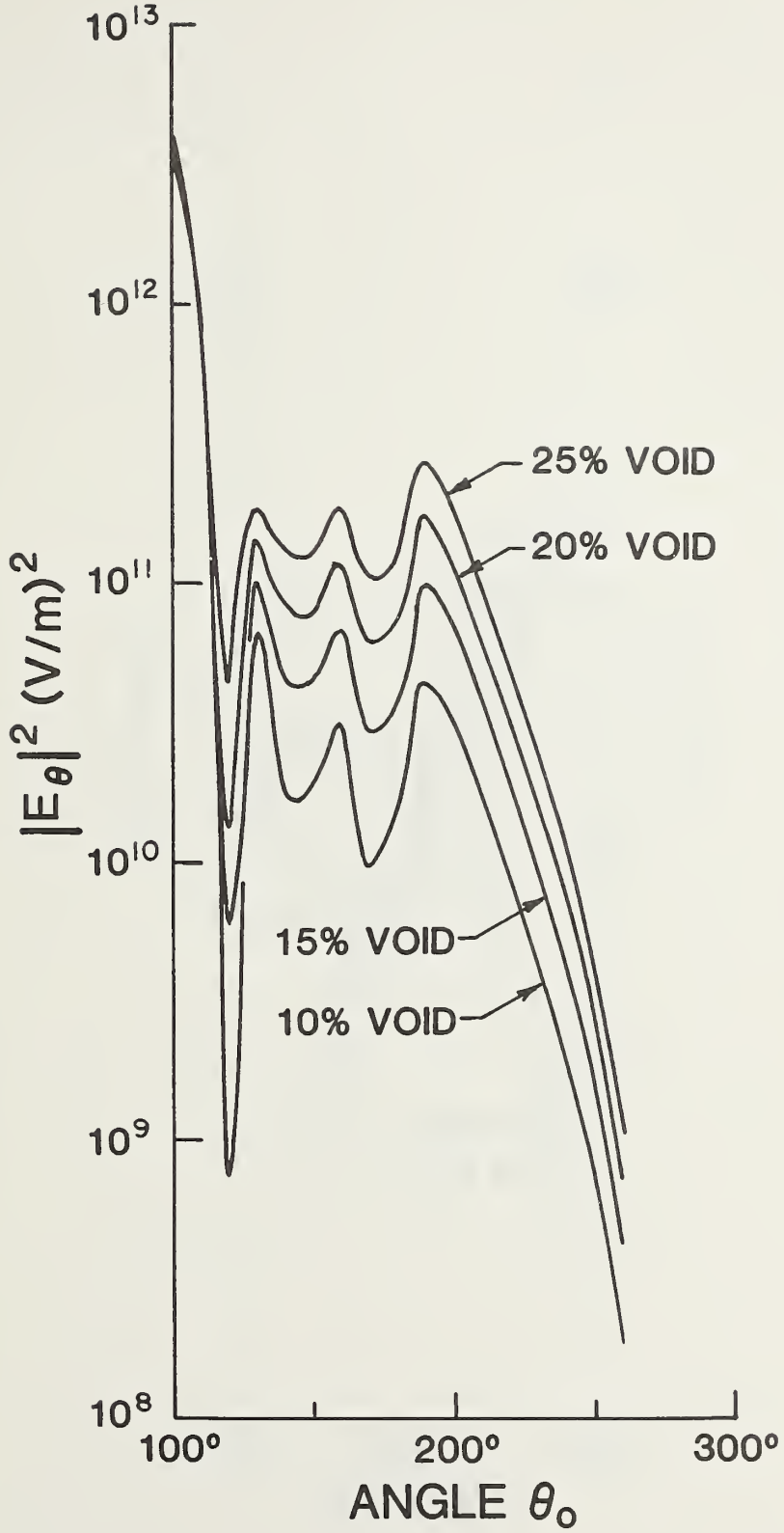


Figure 4. $|E_\theta|^2$ vs scattering angle; dipole along x-axis.

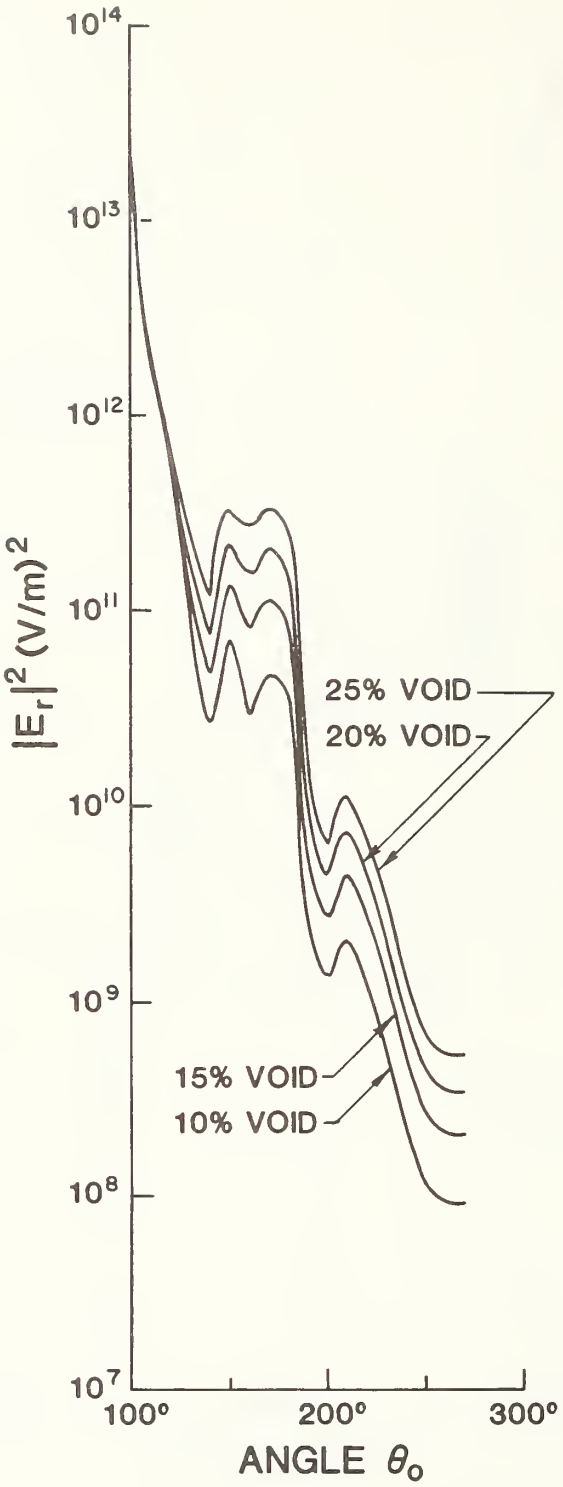


Figure 5. $|E_r|^2$ vs scattering angle; dipole along x-axis.

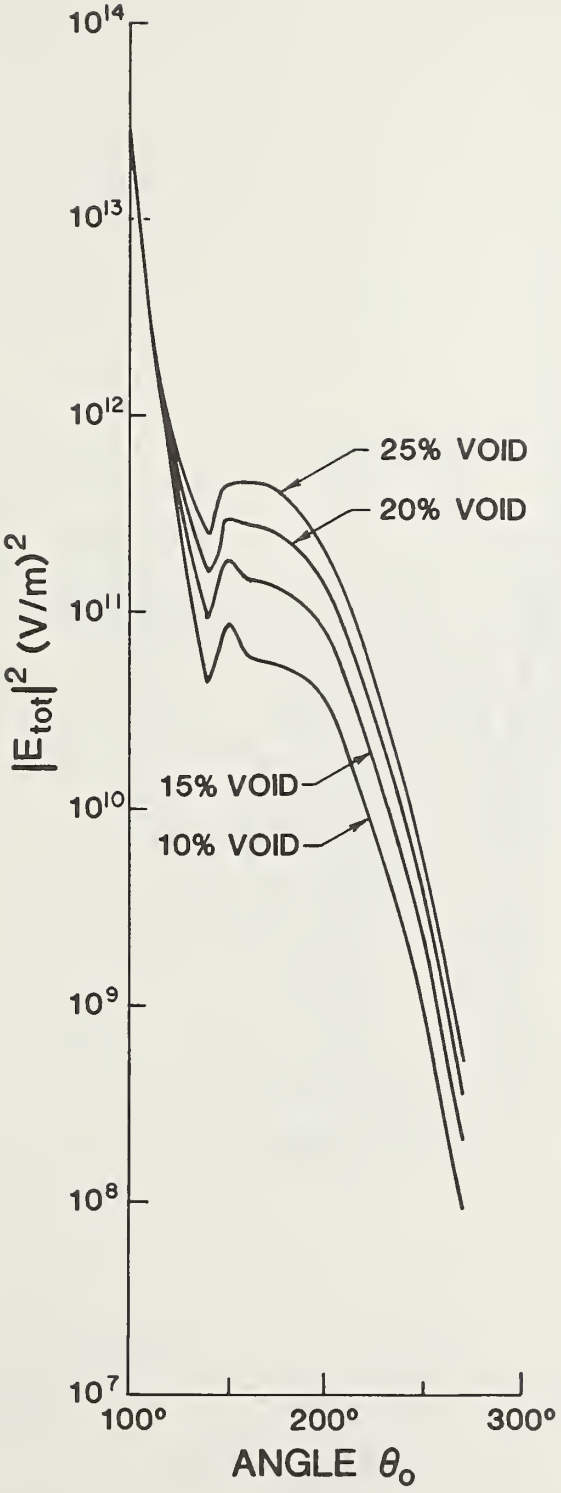


Figure 6. $|\vec{E}_{tot}|^2$ vs scattering angle; dipole along x-axis.

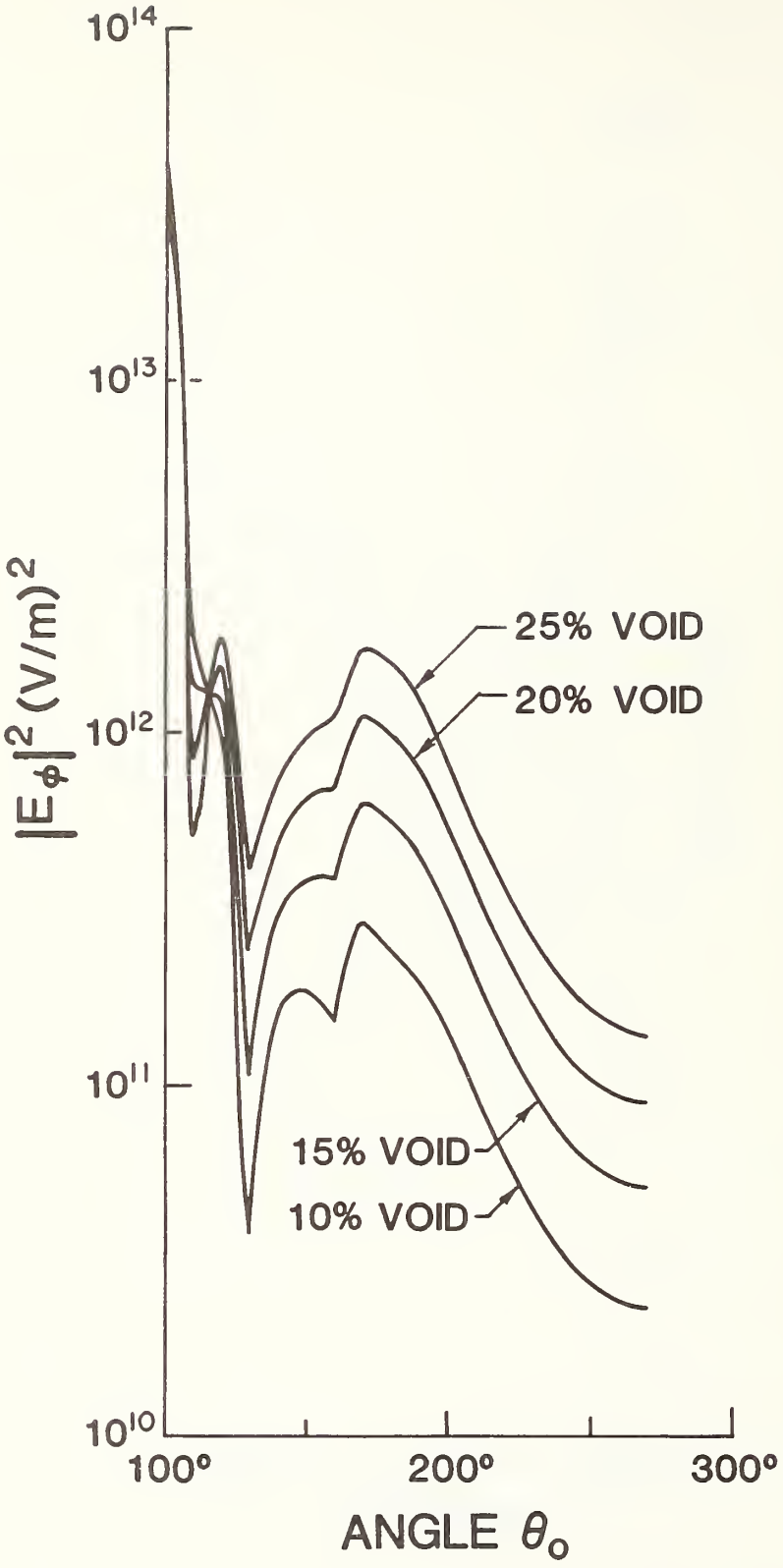


Figure 7. $|E_\phi|^2$ vs scattering angle; dipole along y-axis.

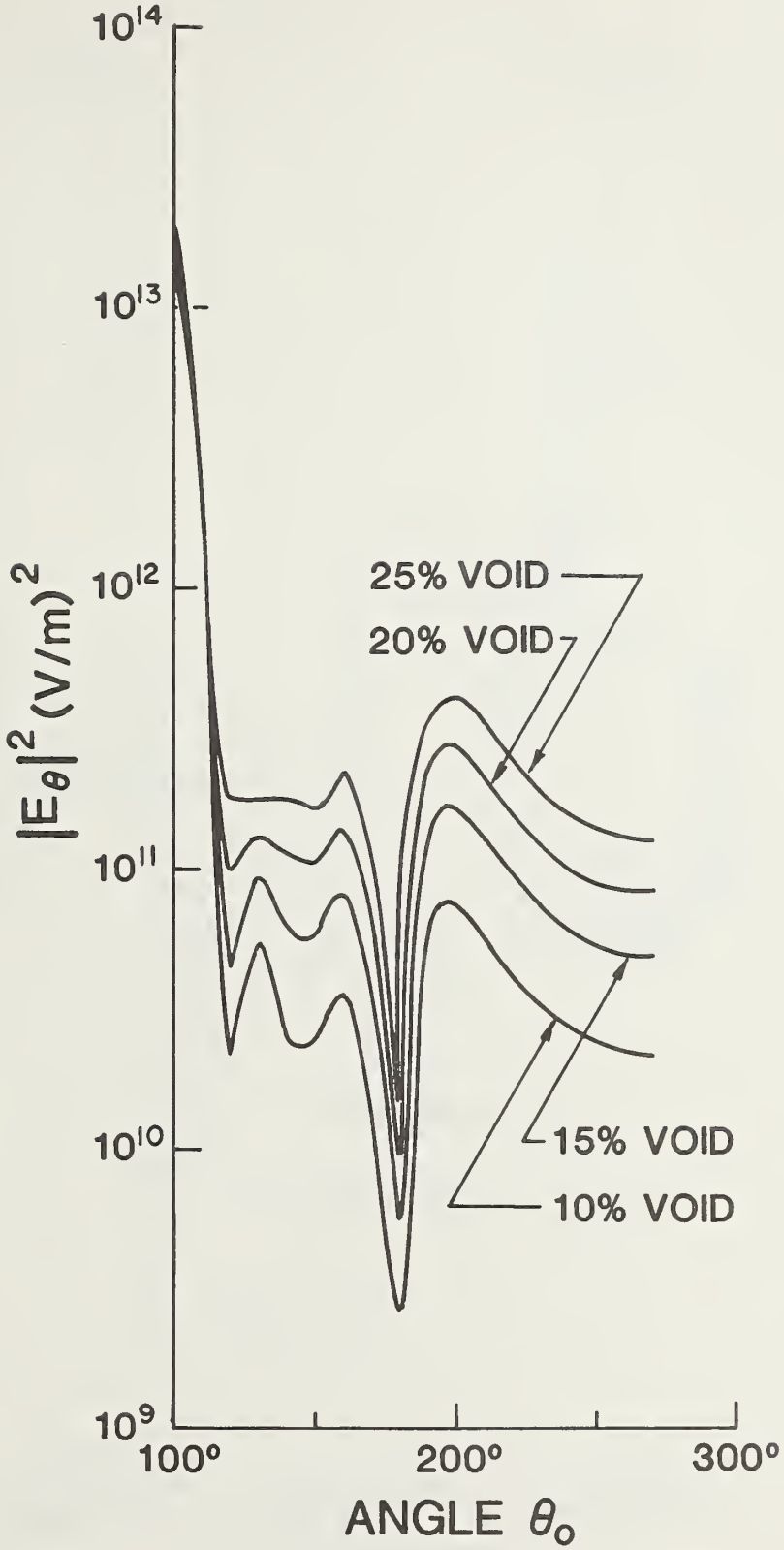


Figure 8. $|E_\theta|^2$ vs scattering angle; dipole along z-axis.

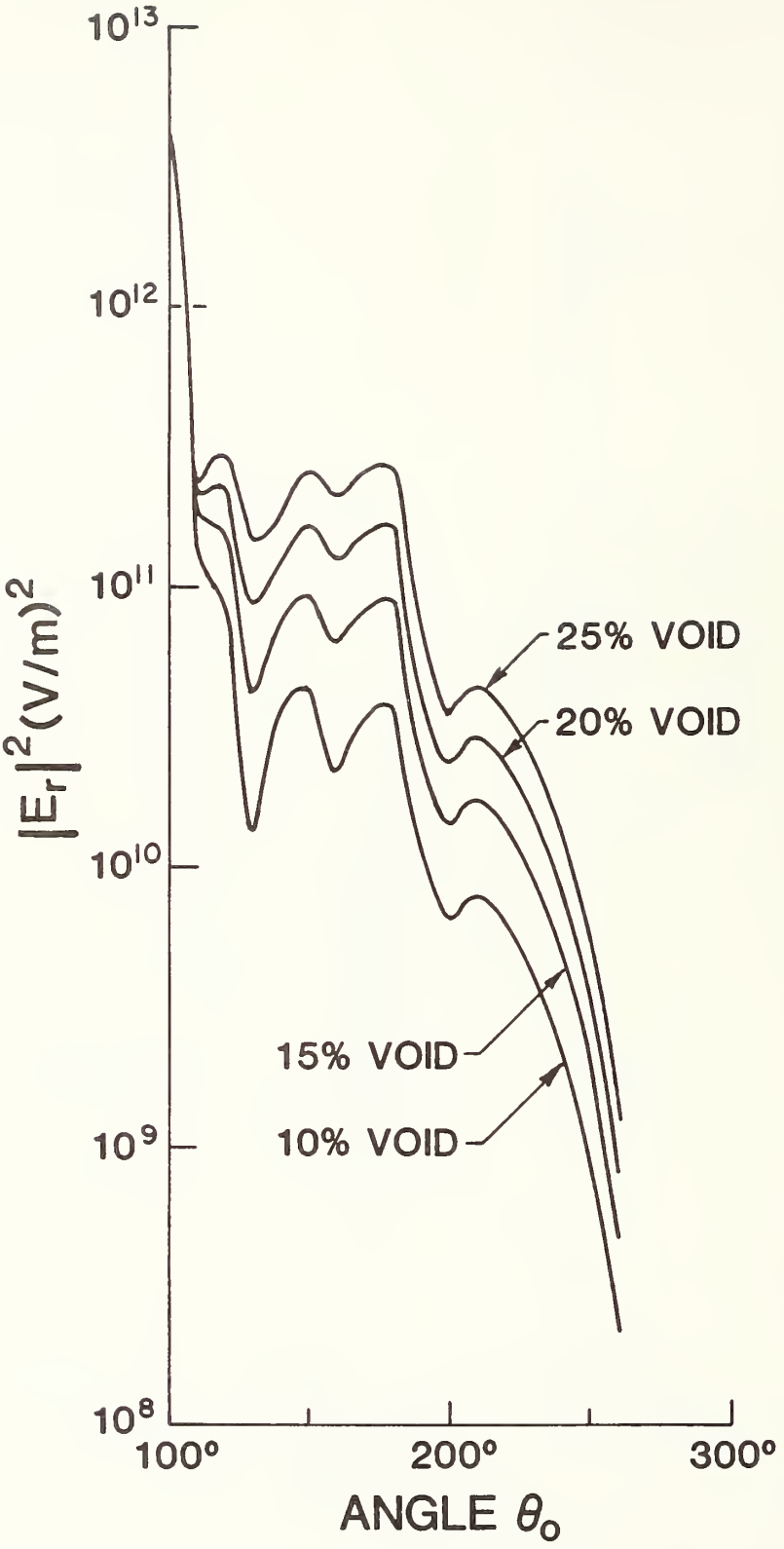


Figure 9. $|E_r|^2$ vs scattering angle; dipole along z-axis.

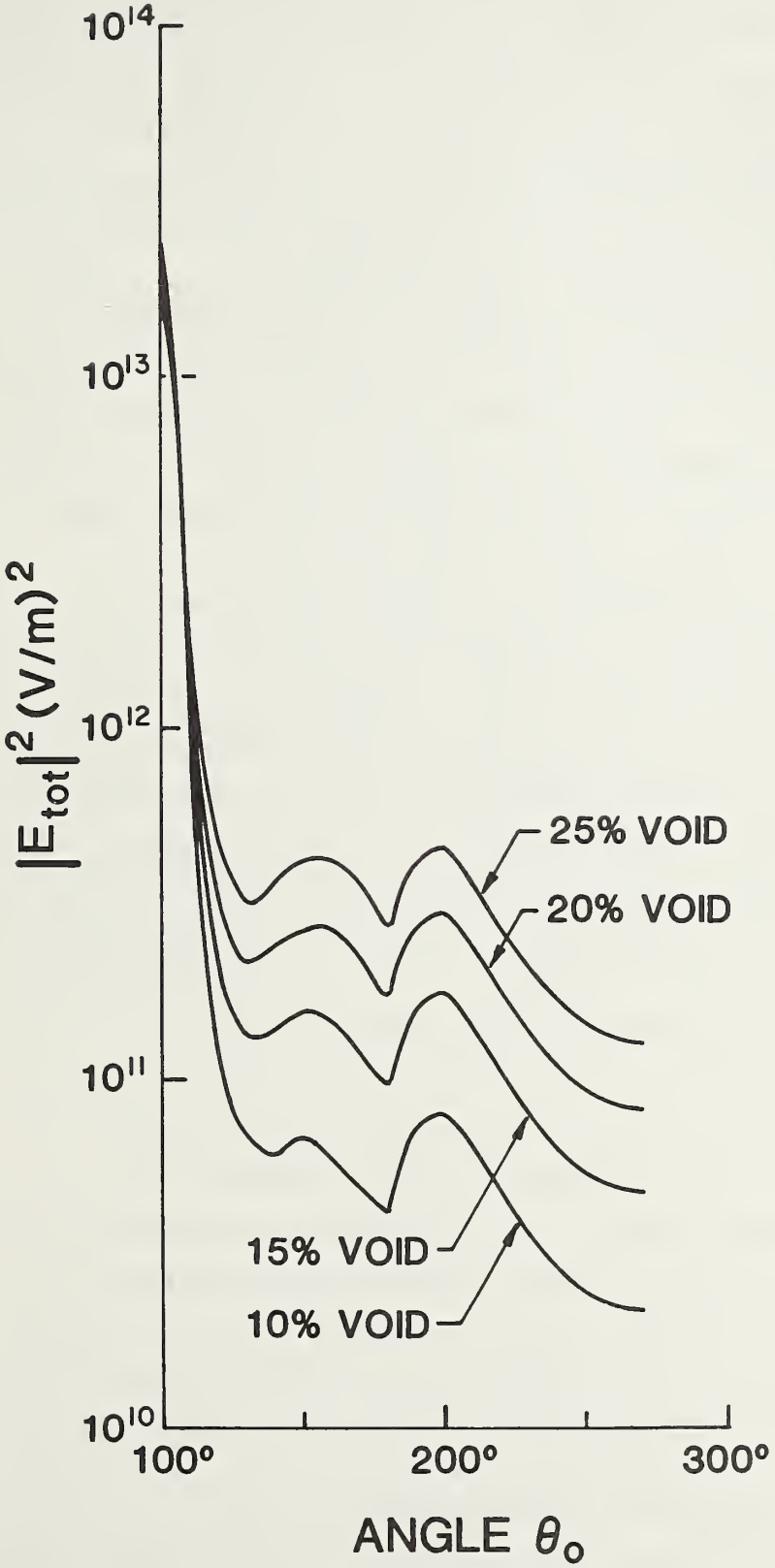


Figure 10. $|\vec{E}_{tot}|^2$ vs scattering angle; dipole along z-axis.

there is primarily the scattered field, which has travelled a much shorter distance and therefore suffered less attenuation. It will also be noted that on the far side, where the scattered field is dominant, the field intensity increases with the void ratio. This is to be expected because a larger void ratio means a greater difference between the dielectric constants inside and outside, which in turn causes more scattering. This is also true for the spherical case, as can be seen from the factor $\varepsilon_1 - \varepsilon_2$ in eq (A2). For the cases shown, a 5% change in the void ratio changes the output intensity by roughly a factor of two for most angles on the far side. There is thus hope that the void ratio can be determined with some accuracy by measurement of the output intensity, provided the bulk dielectric constant is known accurately. This is also limited by the accuracy of the Lichtenecker formula, for which more measurements with shale rocks would be desirable.

The numerical results presented here were obtained on the CDC Cyber 750 computer at NOAA, Boulder. The general description of the program and program listing is given in appendices 2 and 3 respectively. For each dipole orientation and fixed values of the dielectric constants at 4 MHz, it took approximately 200 seconds to compute the squares of the components of the fields over the whole angular range. For higher frequencies or larger dielectric constants, both the number of terms needed (and therefore the matrix rank in the solution of eqs (7) and (9)) and the number of integration sections for the surfaces integrals (8) must be increased, thereby driving up the computer time and storage capacity needed steeply.

## IV. CONCLUSIONS AND RECOMMENDATIONS

The present work suggests the possibility of determining the void ratio of an oil shale retort by remote electromagnetic measurements under suitable conditions. When the shale rock is highly lossy, the source field is largely damped out on the side of the retort away from the transmitter, so the field there consists mainly of the scattered field. This field depends sensitively on the void content of the retort and thus provides a useful tool for the extraction of information on the contents of the retort. In practice, an average dielectric constant for the inside of the retort may be determined using the observed signals and the void ratio obtained from the average dielectric constant with the help of relations like Lichtenecker's formula. In the cases studied here, a small increase in the void ratio produces a

significant increase in the intensity of the scattered field. This circumstance is very helpful in deducing the void ratio from the intensity measurements. However, many assumptions and approximations are involved in this approach, and limitations due to some of them are discussed below.

(1) Geometric approximations. After blasting, the sharp edges and corners of the retort are expected to be rounded off and the retort can probably be adequately modelled by a spheroid. Perturbation methods are available to handle small departures from spheroidal geometry, but additional physical measurements will be needed to characterize the departures and considerably more programming and computer time will be needed. We have not been able to ascertain the effects of neglecting the boreholes.

(2) Limitations due to the approximate nature of the relation between the dielectric constant and the void ratio. This is a sticky question and we have little to add to the existing literature. The Lichtenecker relation is used here partly because of its simplicity, and it is in approximate agreement with all the relevant data we are aware of. There is also another technical advantage. In the Lichtenecker formula, eq (1a), the void ratio $V_1/V$ is to be found from the measured values of $\varepsilon$ and $\varepsilon_2$. Because only the logarithms of $\varepsilon$ and $\varepsilon_2$ enter the equation, error in $\varepsilon$ and $\varepsilon_2$ will tend to be suppressed, giving a good determination of $V_1/V$. We believe more experiments with accurate volume measurements on the relevant shale rocks at the operating frequencies will be helpful.

(3) Possible presence of moisture, etc. The determination of the void ratio from the measured signals in this model depends on the assumption that the content of the retort consists of rubble and void. Because water has a large dielectric constant even at quite high frequencies, a small amount of moisture may change the average dielectric constant significantly and complicate the interpretation of the data. This is a serious potential problem. The presence of pyrites would cause similar problems. Although there is no difficulty in handling magnetic media in our approach, an unknown amount of magnetic material would introduce additional uncertainty to the analysis of the signals.

(4) Computer time. Even at 4 MHz, the amount of computer time needed to generate the data presented here ran into hundreds of seconds for each void ratio and dipole orientation. Mainly for this reason, we have not fully explored the nature of the signal as a function of transmitter orientation, or

the effects of phase differences between the components of the dipole source, etc. For general orientation of the dipole source, the field intensity will not have the symmetry with respect to 90° and 270° in figures 4-10. It is possible that certain orientations may be particularly favorable for the determination of the void ratio. In the cases studied here, it appears that the total intensity for $\theta_0 > 180^0$ (figure 10) with a dipole source oscillating vertically provides clearer separation between the curves corresponding to different void ratios.

ACKNOWLEDGMENTS

The author would like to thank Mr. Doyle Ellerbruch and his group for their hospitality at the NBS, Boulder, and for his kind permission for the use of figure 1. He would also like to thank Profs. P. Barber and D.S. Wang for making available to him important parts of the program and for invaluable advice in the programming. The generous help of the NOAA computing staff and Ms. J. Page's expert word processing are also gratefully acknowledged.

## REFERENCES


[1] Waterman, P.C. Matrix methods in potential theory and electromagnetic scattering. J. App. Phys. 50: 4550-4566; 1979. This paper contains references to earlier work on the EBCM.

[2] Barber, P.; Yeh, C. Scattering of electromagnetic waves by arbitrarily shaped dielectric bodies. App. Optics 14: 2864-2872; 1975.

[3] Jesch, R. Private communication.

[4] For a recent review see, for example: Lamb, W; Wood, D.M.; Ashcroft, N.W. Long-wavelength electromagnetic propagation in heterogeneous media. Phys. Rev. B21: 2248-2266; 1980.

[5] For a review of works more closely related to our problem see: Warne, L.K.; Uhl, J.E. Preliminary study of the remote sensing of a modified in situ oil shale retort by electromagnetic methods. Sandia Report SAND79-1988; 1980 March. 92 p.

[6] Earlier literature, including Lichtenecker's work, is summarized in: von Hippel, A. Dielectrics and waves. New York: John Wiley and Sons; 1954. 284 p.

[7] Sillars, R.W. The properties of a dielectric containing semiconducting particles of various shapes. J. Instr. Elect. Eng. (London) 80: 378-394; 1937.

[8] Bussey, H.; Roop, D. Private communication.

[9] Chew, H.; Kerker, M.; Cooke, D. Electromagnetic scattering by a dielectric sphere in a diverging radiation field. Phys. Rev. 16A: 320-323; 1977.

[10] Edmonds, A.R. Angular momentum in quantum mechanics. New Jersey: Princeton University Press; 1974. 146 p.

[11] Abramowitz, M.; Stegun, I.A., eds. Handbook of mathematical functions. Nat. Bur. Stand. (U.S.); 1965. 1046 p.

[12] Stratton, J.A. Electromagnetic theory. New York: McGraw-Hill Book Co.; 1942. 615 p.

## APPENDIX 1.

This appendix gives the derivation of the Rayleigh limit of the scattered field for a spherical retort referred to in the Introduction.

For a spherical retort of radius a, analytical expressions can be found for the near field when the frequency is sufficiently low so that $ka = 2\pi a/\lambda$ ($\lambda$ = wavelength) is small compared to unity. They can be obtained from the results of Chew, Kerker, and Cooke [9] generalized to absorbing media by expanding the field coefficients in powers of ka and retaining only the lowest order terms.

Let the retort be centered at the origin and the coordinate axes chosen so that the dipole source (dipole moment $\vec{P}$) lies outside the retort at cartesian coordinates (0, 0, -d) (d>a). We expand the scattered field in a series of vector spherical harmonics in the notation of [9]:

$$\vec{E}_{sc}(\vec{r}) = \sum_{\ell=1}^{\infty} \sum_{m=-\ell}^{m=\ell} \{\frac{ic}{n_2^2\omega} \beta_E(\ell,m) \nabla x [h_\ell^{(1)}(k_2 r) \vec{Y}_{\ell\ell m}(\hat{r})]$$

$$+ \beta_M(\ell_1 m) h_\ell^{(1)}(k_2 r) \vec{Y}_{\ell\ell m}(\hat{r})\}. \qquad (A1)$$

Here, $\vec{Y}_{\ell\ell m}(\hat{r})$ denotes a vector spherical harmonics as defined in Edmonds [10], $h_\ell^{(1)}(x)$ denotes the spherical Hankel function of the first kind [11], $\omega = 2\pi f$, $n_2$ and $k_2$ being the complex index of refraction and wave number in the (outside) medium 2. It is then shown in [9] that the expansion coefficients are given by

$$\beta_E(\ell_1 m) = -b_\ell a^d{}_E(\ell_1 m),$$

$$\beta_M(\ell_1 m) = -a_\ell a^d{}_M(\ell_1 m),$$

where $a_\ell$ and $b_\ell$ are Mie scattering coefficients as defined in Stratton [12], and the only nonvanishing $a^d_E$'s and $a^d_M$'s in our case are

$$a^d{}_E(\ell_1 \pm 1) = \pm jk_2{}^3\sqrt{\pi}(-1)^\ell(2\ell+1)^{-1/2} (P_x \pm jP_y)[\ell h_{\ell+1}^{(1)}(k_2 d) - (\ell+1)h_{\ell+1}^{(1)}(k_2 d)],$$

$$a^d{}_E(\ell_1 \pm 0) = jk_2{}^3(-1)^\ell P_z[4\pi\ell(\ell+1)(2\ell+1)]^{1/2} h_\ell^{(1)}(k_2 d)/k_2 d,$$

$$a^{d}_{M}(\ell_1 \pm 1) = jk_2^3(-1)^{\ell}[\pi(2\ell+1)]^{1/2}(P_x \pm jP_y)\, h_{\ell}^{(1)}(k_2 d).$$

Making the small ka expansion indicated above, we find for the leading terms in the expansion

$$\vec{E}_{sc}(\vec{r}) = -\frac{2}{3} \cdot \frac{n_2^4 \omega^5 a^3}{c^2} \cdot \frac{\varepsilon_1 - \varepsilon_2}{\varepsilon_1 + 2\varepsilon_2} \cdot \{[h_2^{(1)}(k_2 d) - 2h_0^{(1)}(k_2 d)]$$

$$[\frac{(rh_1^{(1)}(k_2 r))'}{2r}((P_x \cos\phi - P_y \sin\phi)\cos\theta\hat{\theta} - (P_x \sin\phi + P_y \cos\phi)\hat{\phi})$$

$$+ \frac{h_1^{(1)}(k_2 r)}{r}(P_x \cos\phi - P_y \sin\phi)\sin\theta\, \hat{r}] + 3P_z \frac{h_1^{(1)}(k_2 d)}{k_2 d}$$

$$(\frac{(rh_1^{(1)}(k_2 r))'}{r} \sin\theta\hat{\theta} - \frac{2h_1^{(1)}(k_2 r)\cos\theta}{r}\hat{r})\}, \qquad \text{(A2)}$$

where $(r, \theta, \phi)$ denote the spherical coordinates of the receiver, the prime indicates derivative with respect to r, $\varepsilon_1$, $\varepsilon_2$ denote the complex dielectric constants inside and outside respectively, and $n_2$ denotes the complex refractive index of the external medium. For an oil shale retort, where the void ratio is typically of the order of 15 percent, $\varepsilon_1$ does not differ very much from $\varepsilon_2$ and the factor $\varepsilon_1 - \varepsilon_2$ is a sensitive function of the void ratio. If the medium outside is highly absorbing, then on the side of the retort away from the source the total field is dominated by the scattered field $\vec{E}_{sc}$. Thus, measurment of the field there will provide valuable information about the void ratio.

## APPENDIX 2.

This appendix contains a general description of the program and instructions for its use.

The program computes the incident field coefficients, the elements of the T-matrix, and from these the scattering coefficients. Two subroutines, GENBKR and GENLGP, generate the necessary spherical Bessel functions of complex arguments and Legendre functions. Subroutine GAUSS carries out the numerical integration over the spheroid surface to give the needed matrix elements. After the scattering coefficients are calculated, they are multiplied by the appropriate Bessel and Legendre functions of the receiver coordinates to give the spherical components $E^{sc}_{\theta}$, $E^{sc}_{\phi}$, and $E^{sc}_{r}$ of the scattered field. The dipole source has been taken, without loss of generality, to be in the x-z plane with spherical coordinates ($r_d$, $\theta_d$, $\phi_d = 0$). The scattered field is calculated in the vertical plane $\phi_0$ = constant (taken to be zero in the program listed in Appendix 3) for a fixed radial coordinate $r_0$ (taken to be 1.1a in Appendix 3), while the angle $\theta_0$ is varied from 0° in steps of $\Delta\theta$ (denoted by DLTANG and with the value 10° in Appendix 3) up to 360°. At each angle subroutine DIPOLE computes the dipole field due to the same source and adds it to the scattered field to form the spherical components of the total near field $E^{tot}_{\theta}$, $E^{tot}_{\theta}$, $E^{tot}_{r}$. Finally, the program computes and prints $|E^{tot}_{\theta}|^2$ $|E^{tot}_{\theta}|^2$, $|E^{tot}_{r}|^2$, and $|\vec{E}^{r}_{tot}|^2 = |E^{tot}_{\theta}|^2 + |E^{tot}_{\phi}|^2 + |E^{tot}_{r}|^2$ as functions of the scattering angle $\theta_0$ (denoted by SCANG in Appendix 3). The geometry is shown in figure 3.

Following is a list of the input quantities needed to obtain numerical results:

1. The real and imaginary parts of the dielectric constants inside and outside the retort, denoted by DCNR, DCNI; DCNR2, DCNI2, respectively.

2. The frequency. This is expressed in terms of the vacuum wave number WN = $k_0 = 2\pi f/c$ in the input.

3. The size parameter $k_0 a = 2\pi fa/c \equiv$ CONK (a = major axis of the spheroid, which is taken to be prolate in Appendix 3), and the ratio of the spheroidal axes a/b (denoted by AOVRB).

4. The radial coordinates of the dipole transmitter ($r_d$) and of the receiver ($\theta_0$).

a. In subroutine DIPOLE, $r_d$(≡RD) is entered as $(r_d/a)\cdot(k_0a/k_0)$, or RD = $(r_d/a)$*CONK/WN, $r_d/a$ being taken to be 1.05 in Appendix 3. The coordinate $r_0$ (denoted by RO) is entered as $(r_0/a)\cdot a = (r_0/a)\cdot(k_0a/k_0)$, or RO = $(r_0/a)$*CONK/WN, with $r_0/a$ being set equal to 1.1 in the program. Both $r_0/a$ and $r_d/a$ may be set at any value > 1. However, if $r_0 < r_d$, it will be necessary to make the interchange of Bessel and Hankel functions indicated in section III.

b. In subroutine ADDPRC, they are entered through the arguments of the radial functions $\rho'$(≡RHOP) = $(r_d/a)\cdot k_2a = (r_d/a)$ $k_0a\sqrt{\varepsilon_2} = (r_d/a)$ *CONK*CSQRT(DCN2), and $\rho$(≡RHO) = $(r_0/a)\cdot k_2a = (r_0/a)$ *CONK*CSQRT(DCN2).

5. The angular coordinates of the transmitter $\theta_d$ ≡ THETAD, $\phi_d$ being set equal to zero, and the azimuthal angle of the receiver $\phi_0$ ≡ PH. They are given the values THETAD = 90° and PH = 0 in Appendix 3.

6. The cartesian components of the dipole moment $P_x$ = PX, $P_y$ = PY, $P_z$ = PZ. These are allowed to be complex so that phases between the components may be introduced. They have to be entered in both subroutines ADDPRC and DIPOLE.

7. The number of values of m (Nm) and n (NRANK).

8. The number of sections used in the integration over the spheroid surface (NDPS).

9. The angular increment (denoted by DLTANG) in the scattering angle (denoted by SCANG), and the number of angles for which the squares of the field components are calculated. The last quantity is denoted by NUANG and is equal to 360°/DLTANG + 1.

Most of these input quantities are entered on four data cards at the end of the program (see listing, Appendix 3).

The first card lists Nm, NRANK, and three numbers (1,8,1) which are to be left alone.

The second card lists CONK, AOVRB, WN, DCNR, DCNI.

The third card gives NDPS.

The fourth card lists THETAD, PH, DCNR2, DCNI2, DLTANG, NUANG.

The data on these cards must be entered so that the last digit of the first entry is on the 12th space, the second on the 24th space, the third on the 36th space, etc. These data are read by subroutine RDDATA and stored in various common blocks for use in the other subroutines.

## APPENDIX 3. Listing of the Program

```
      PROGRAM SHALE (INPUT,OUTPUT,TAPE 5 = INPUT,TAPE 6 = OUTPUT)
      COMPLEX A,B,DCN,SQ,QS,RH,RR(40),HBK,BBK,HEPS,REPS,S,SQR,QSR,BKK,
     1HTBKK,RTBKK,SA1,SB1,SQR2,D,CCC,BSSLSP(41),CNEUMN(41),RBESSL(40),
     2SQ2,QS2,DCN2,CI,BR,HH,CCKP,CIKP,DCKK,BSLCMP,CNEUM,ACANSR
C     PERFORM THE NUMERICAL INTEGRATION AND FILL THE A AND B MATRICES.
      COMMON DTR,RTD,CPI
      COMMON /MTXCOM/ NRANK,NRANKI,A(80,80),B(80,80),CMXNRM(80)
      COMMON /ENGCOM/ PNMLIG(41),BSLCMP(41),CNEUM(41),BSLKPR(41),BSLKPI
     1(41)
      COMMON /CMVCOM/ NM,KMV,CMI(40),CMV,CM2,TWM,PRODM
      COMMON /BDYCOM/ DCNR,DCNI,CKPRR,CKPRI,CKR,DCKR,CONK,AOVRR,WN,IB
      COMMON /THTCOM/ THETA,SINTH,COSTH,CDH(6),EPPS(6),NSECT,NDPS(6)
     1,THETAD,PH,KSECT
      COMMON/UVCCOM/ACANS(361,2,2),ACANSR(361),DLTANG,DCNR2,DCNI2,NUANG
      DIMENSION CLRMTX(25600),CLRTOT(1444),RH(40),WT(300),ASC(300)
      EQUIVALENCE (A(1,1),CLRMTX(1)),(ACANS(1,1,1),CLRTOT(1))
C     SET PROGRAM CONSTANTS.
      CI = (0.0,1.0)
      DTR =.017453292519943
      RTD = 57.2957795131
      CPI = 3.1415926535898
C     CALL ROUTINE TO READ DATA AND PRINT HEADINGS FOR OUTPUT
   20 CALL RDDATA
C     CLEAR THE ACCUMULATING ANSWER REGISTER (USED IN ADDPRC).
      DO 40 J=1,1444
      CLRTOT(J) = 0.0
   40 CONTINUE
      DO 41 J=1,361
      ACANSR(J) = 0.0
   41 CONTINUE
      DCN2 = CMPLX(DCNR2,DCNI2)
      SQ2 = CSQRT(DCN2)
      QS2 = 1.0/SQ2
      DCN = CMPLX(DCNR,DCNI)
      SQR = CSQRT(DCN/DCN2)
      QSR = 1.0/SQR
      SQR2 = SQR*SQR
      SQ = CSQRT(DCN)
      QS = 1.0/SQ
C     SET MULTIPLIER B89 DEPENDENT ON IB VALUE (SYMMETRY INDICATOR).
      B89 = 1.0
      IF(IB.EQ.8) B89=2.0
      BDYFCT = 1.0
C     SET UP A LOOP FOR EACH M VALUE.
      DO 900 IM = 1,NM
C     SET M DEPENDENT VARIABLES.
```

```
      CMV = CMI(IM)
      KMV = CMV
      CM2 = CMV**2
      PRODM = 1.0
      IF(KMV.GT.0) GO TO 44
      EM = 1.0
      GO TO 60
   44 EM = 2.0
      QUANM = CMV
      DO 52 IFCT = 1,KMV
      QUANM = QUANM+1.0
      PRODM = QUANM*PRODM/2.0
   52 CONTINUE
   60 QEM = 2.0/EM
      TWM = 2.0*CMV
C     INITIALIZE ALL MATRIX AREAS TO ZERO
      DO 80 I = 1,25600
      CLRMTX(I) = 0.0


   80 CONTINUE
C     SET UP A LOOP FOR ALL VALUES OF THETA.
C     SET UP GENERAL LOOP FOR CORRECT NUMBER OF INTEGRATION SECTIONS.
      DO 800 ISECT = 1,NSECT
      KSECT = ISECT
      NTHETA = NDPS(ISECT)
      IF(ISECT.EQ.1) CALL GAUSS(WT,ASC,NTHETA,0.0,EPPS(ISECT))
      IF(ISECT.NE.1) CALL GAUSS(WT,ASC,NTHETA,EPPS(ISECT-1),EPPS(ISECT))
C     ENTER THETA LOOP FOR EACH SECTION.
      DO 700 ITHTA = 1,NTHETA
      THETA = ASC(ITHTA)
      COSTH = COS(THETA)
      SINTH = SIN(THETA)
C     GENERATE THE LEGENDRE POLYNOMIALS.
      CALL GENLGP
C     EVALUATE KR AND ITS DERIVATIVE AS A FUNCTION OF THETA.
  348 CALL GENKR
C     GENERATE ALL NECESSARY BESSEL AND NEUMANN FUNCTIONS AND THEIR RATIOS.
      CKPRR = REAL(SQ2*CKR)
      CKPRI = AIMAG(SQ2*CKR)
      CALL GENBKR
      CCKP = CMPLX(CKPRR,CKPRI)
      CIKP = 1.0/CCKP
      DCKK = SQ2*DCKR
      DO 349 I=1,NRANKI
      BSSLSP(I) = BSLCMP(I)
      CNEUMN(I) = CNEUM(I)
  349 CONTINUE
      CKPRR = REAL(SQ*CKR)
      CKPRI = AIMAG(SQ*CKR)
      CALL GENBKR
      IF(ITHTA .NE.NTHETA) GO TO 79
   79 CONTINUE
      DO 350 K = 1,NRANK
```

```
      RRESSL(K) = RSSLSP(K)/RSSLSP(K+1)
      RH(K) = (RSSLSP(K)+CI*CNEUMN(K))/(RSSLSP(K+1)+CI*CNEUMN(K+1))
      RR(K)=SQR*CMPLX(RSLKPR(K),RSLKPI(K))/CMPLX(RSLKPR(K+1),RSLKPI(K+1)
     1)
  350 CONTINUE
      SRMSIN = WT(ITHTA)*SINTH
C     SET UP A LOOP FOR EACH ROW OF THE MATRICES.
      CROW = 0.0
      CROWM = CMV
      DO 600 IROW = 1,NRANK
      IROW1 = IROW+NRANK
      CROW = CROW+1.0
      CROWM = CROWM+1.0
      CROW1=CROW+1.0
      RR = RRESSL(IROW)
      HH = RH(IROW)
C     SET UP A LOOP FOR EACH COLUMN OF THE MATRICES.
      CCOL = 0.0
      CCOLM = CMV
      DO 400 ICOL = 1,NRANK
      ICOL1 = ICOL+NRANK
      CCOL = CCOL+1.0
      CCOLM = CCOLM+1.0
      CCOL1 = CCOL+1.0
C     CALCULATE FREQUENTLY USED VARIABLE COMBINATIONS.
      CRIJ = CROW+CCOL
      CRSSIJ = CROW*CCOL
      CMCRCO = CM2+QEM*CRSSIJ*COSTH**2
      PNROCO = PNMLLG(IROW)*PNMLLG(ICOL)
      PNROC1 = PNMLLG(IROW)*PNMLLG(ICOL+1)


      PNR1CO = PNMLLG(IROW+1)*PNMLLG(ICOL)
      PNR1C1 = PNMLLG(IROW+1)*PNMLLG(ICOL+1)
      R1A = CROW*COSTH*PNR1C1-CROWM*PNROC1
      R1B = CCOL*COSTH*PNR1C1-CCOLM*PNR1CO
      RKK = RR(ICOL)
      HRK=(RSSLSP(IROW+1)+CI*CNEUMN(IROW+1))*CMPLX(RSLKPR(ICOL+1),RS
     1LKPI(ICOL+1))
      RRK = RSSLSP(IROW+1)*CMPLX(RSLKPR(ICOL+1),RSLKPI(ICOL+1))
      HEPS = QSR*HRK
      REPS = QSR*RRK
      IF(IB.EQ.9) GO TO 380
C     IF IB = 8 (MIRROR SYMMETRY BODY), I=L=0 IF IROW AND ICOL ARE BOTH
C     ODD OR BOTH EVEN, J=K=0 IF IROW AND ICOL ARE ODD,EVEN OR EVEN,ODD.
      IF((IROW+ICOL).EQ.((IROW+ICOL)/2)*2) GO TO 392
C     TEST FOR M=0 (IF M=0 THE I AND L SUBMATRICES ARE ZERO).
  380 IF(KMV.EQ.0) GO TO 390
C
C     CALCULATE THE K,L,I,J AND K,L,I,J (PRIME) MATRIX ELEMENTS AND PLACE
C     THEM IN THE A AND B MATRICES RESPECTIVELY SO AS TO FORM A-TRANSVERSE
C     AND B-TRANSVERSE MATRICES.
C
C     CALCULATE THE TERM FOR THE CURRENT ELEMENT IN THE I MATRIX.
C
```

```
      B1 = B1A+B1B
      HTBKK = HH*BKK
      BTBKK = BB*BKK
      SA1 = PNR1C1*(CROW*CROW1*BKK+CCOL*CCOL1*HH-CRSSIJ*(CRIJ+2.0)*CIKP)
     1*DCKK*SINTH
      S=SA1+(CCKP*(1.0+HTBKK)-CCOL*HH-CROW*BKK+CRSSIJ*CIKP)*B1*CCKP
      A(ICOL,IROW1)  =A(ICOL,IROW1)  +B89*CMV*SRMSIN*S*HBK
      SB1 = PNR1C1*(CROW*CROW1*BKK+CCOL*CCOL1*BB-CRSSIJ*(CRIJ+2.0)*CIKP)
     1*DCKK*SINTH
      S=(CCKP*(1.0+BTBKK)-CCOL*BB-CROW*BKK+CRSSIJ*CIKP)*B1*CCKP+SB1
      B(ICOL,IROW1)  =B(ICOL,IROW1)  +B89*CMV*SRMSIN*S*BBK
C
C     CALCULATE THE TERM FOR THE CURRENT ELEMENT IN THE L MATRIX.
C
      S=(CCKP*(SQR2+HTBKK)-CCOL*HH-CROW*BKK+CRSSIJ*CIKP)*B1*CCKP+SA1
      A(ICOL1,IROW)  =A(ICOL1,IROW)  -B89*CMV*SRMSIN*S*HEPS
      S=(CCKP*(SQR2+BTBKK)-CCOL*BB-CROW*BKK+CRSSIJ*CIKP)*B1*CCKP+SB1
      B(ICOL1,IROW)  =B(ICOL1,IROW)  -B89*CMV*SRMSIN*S*BEPS
  390 IF(IB.EQ.8) GO TO 400
C
C     CALCULATE THE TERM FOR THE CURRENT ELEMENT IN THE J MATRIX.
C
  392 A12=CMCRCO*PNR1C1-QEM*(CROW*CCOLM*COSTH*PNR1CO+CCOL*CROWM*COSTH*PN
     1ROC1-CROWM*CCOLM*PNROCO)
      B1A = CCOL*CCOL1*B1A
      B1B = CROW*CROW1*B1B
      D = QEM*DCKK
      CCC = SQR2*HH
      S=(CCKP*(BKK-CCC)+SQR2*CROW-CCOL)*A12*CCKP+(B1A-SQR2*B1B)*SINTH*D
      A(ICOL1,IROW1)  =A(ICOL1,IROW1)  +B89*SRMSIN*S*HEPS
      CCC = BB*SQR2
      S=(CCKP*(BKK-CCC)+SQR2*CROW-CCOL)*A12*CCKP-(SQR2*B1B-B1A)*SINTH*D
      B(ICOL1,IROW1)  =B(ICOL1,IROW1)  +B89*SRMSIN*S*BEPS
C
C     CALCULATE THE TERM FOR THE CURRENT ELEMENT IN THE K MATRIX.
C
      B1 = (B1A-B1B)*SINTH
      S = (CCKP*(BKK-HH)+CROW-CCOL)*A12*CCKP+B1*D
      A(ICOL,IROW)  =A(ICOL,IROW)  +B89*SRMSIN*S*HBK
      S = (CCKP*(BKK-BB)+CROW-CCOL)*A12*CCKP+B1*D
      B(ICOL,IROW)  =B(ICOL,IROW)  +B89*SRMSIN*S*BBK


  400 CONTINUE
C     CALCULATE THE NORMALIZATION FACTOR (USED IN ADDPRC).
      CKROW = IROW
      IF(KMV.GT.0) GO TO 426
      FCTKI = 1.0
      GO TO 440
  426 IF(IROW.GE.KMV) GO TO 430
      CMXNRM(IROW) = 1.0
      GO TO 600
  430 IBEGT = IROW-KMV+1
      IENDT = IROW+KMV
```

```
      EPROD = IBEGT
      ECTKI = 1.0
      DO 432 LECT = IBECT,IEECT
      ECTKI = ECTKI*EPROD
      EPROD = EPROD+1.0
  432 CONTINUE
  440 CMXNRM(IROW) = 4.0*CKROW*(CKROW+1.0)*ECTKI/(EM*(2.0*CKROW+1.0))
  600 CONTINUE
  700 CONTINUE
  800 CONTINUE
C     PROCESS COMPUTED MATRICES
      CALL PROSSM
  900 CONTINUE
      GO TO 20
      END
      SUBROUTINE GAUSS(WT,ASC,N,AA,BB)
      DIMENSION WT(N),ASC(N)
      DOUBLE PRECISION PI,CONST
      DATA PI,CONST,TOL/3.14159265358979D0,.1486788163570D0,1.E-12/
      DATA C1,C2,C3,C4/.125,-.0807291666,.2460286458,-1.824438767/
      IF(N.NE.1) GO TO 1
      ASC(1) = 0.5773502692
      WT(1) = 1.0
      RETURN
    1 DN = N
      NDIV2 = N/2
      NP1 = N+1
      NNP1 = N*NP1
      APPECT = 1./DSQRT((N+0.5)**2+CONST)
      CON1 = 0.5*(BB-AA)
      CON2 = 0.5*(BB+AA)
      DO 100 K = 1,NDIV2
      R = (K-.25)*PI
      RISQ = 1./(R*R)
      REROOT = R*(1.+RISQ*(C1+RISQ*(C2+RISQ*(C3+C4*RISQ))))
      X = COS(APPECT*REROOT)
  113 PM2 = 1.
      PM1 = X
      DO 110 IN = 2,N
      P = ((2*IN-1)*X*PM1-(IN-1)*PM2)/IN
      PM2 = PM1
  110 PM1 = P
      PM1 = PM2
      AUX = 1./(1.-X*X)
      DER1P = DN*(PM1-X*P)*AUX
      DER2P = (2.*X*DER1P-NNP1*P)*AUX
      RATIO = P/DER1P
      XI = X-RATIO*(1.+RATIO*DER2P/(2.*DER1P))
      IF(ABS(XI-X)-TOL) 111,111,112
  112 X = XI
      GO TO 113
  111 ASC(K) = -X
      WT(K) = 2.*(1.-X*X)/(DN*PM1)**2
```

```
      ASC(NP1-K) = -ASC(K)
  100 WT(NP1-K) = WT(K)
      IF(MOD(N,2).EQ.0) GO TO 114
      ASC(NDIV2+1) = 0.0
      NM1 = N-1
      NM2 = N-2
      PROD = DN
      DO 120 K = 1,NM2,2
  120 PROD = FLOAT(NM1-K)/FLOAT(N-K)*PROD
      WT(NDIV2+1) = 2./PROD**2
  114 DO 130 K = 1,N
      ASC(K) = CON1*ASC(K)+CON2
  130 WT(K) = CON1*WT(K)
      RETURN
      END
      SUBROUTINE RDDATA
C     A ROUTINE TO READ INPUT FOR THE PROGRAM.
      COMPLEX ACANSR
      COMMON /MTXCOM/ NRANK,NRANKI
      COMMON DTR,RTD,CPI
      COMMON /CMVCOM/ NM,KMV,CMI(40),CMV,CM2,TWM,PRODM
      COMMON /THTCOM/ THETA,SINTH,COSTH,CDH(6),EPPS(6),NSECT,NDPS(6)
     1,THETAD,PH,KSECT
      COMMON /BDYCOM/ DCNR,DCNI,CKPRR,CKPRI,CKR,DCKR,CONK,AOVRB,WN,IB
      COMMON/UVCCOM/ACANS(361,2,2),ACANSR(361),DLTANG,DCNR2,DCNI2,NUANG
      COMMON /OUTCOM/ IOUT
      DIMENSION EPDEG(6)
C
C     READ NECESSARY INPUT DATA.
C
C     CARD1 --- NM = NUMBER OF M VALUES,NRANK = N VALUE(MATRIX ORDER),
C     NSECT = NUMBER OF SECTIONS IN THE BODY,IB = SYMMETRY CODE  IB = 8
C     FOR MIRROR SYMMETRY ABOUT THETA = 90 DEGREES,IB = 9 FOR GENERAL
      READ(5,80)          NM,NRANK,NSECT,IB,IOUT
      IF (EOF(5).NE.0) GO TO 190
      NRANKI = NRANK+1
      WRITE(6,88)
      WRITE(6,92) NM,NRANK,NSECT,IB
C
C     CARD 2 --- CONK = KA OF BODY,AOVRB = A/B,RATIO OF MAJOR TO MINOR
C     AXIS,WN = VACUUM WAVE NUMBER USED IN ADDPRC,DCNR = REAL PART OF
C     DIELECTRIC CONSTANT INSIDE, DCNI = IMAGINARY PART OF SAME.
      READ(5,96) CONK,AOVRB,WN,DCNR,DCNI
      IF (EOF(5).NE.0) GO TO 190
      WRITE(6,100)
      WRITE(6,104) CONK,AOVRB,WN,DCNR,DCNI
      DO 5 I=1,40
      CMI(I) = FLOAT(I-1)
    5 CONTINUE
      IF(NM.EQ.1) CMI(1) = 1.0
C
C     CARD 3 --- NDPS = NUMBER OF INTEGRATION DIVISIONS FOR EACH SECTION
C     OF THE BODY (MUST BE A MULTIPLE OF 4).
      READ(5,80) (NDPS(I),I=1,NSECT)
      IF (EOF(5).NE.0) GO TO 190
      WRITE(6,120) (NDPS(I),I=1,NSECT)
```

```
C
C      CARD 4 -------
C      THETAD = THETA OF DIPOLE.
C      PH = AZIMUTHAL ANGLE OF OBSERVATION PLANE.
C      DCNR2 + CI*DCNI2 = COMPLEX DIELECTRIC CONSTANT OUTSIDE.
C      DLTANG = INCREMENT OF SCATTERING ANGLE IN SCATTERING PLANE IN DEGREE
C      NUANG = NO. OF SECTIONS IN SCATTERING PLANE WITH 360 DEGREES
       READ(5,96) THETAD,PH,DCNR2,DCNI2,DLTANG,NUANG


       IF (EOF(5).NE.0) GO TO 190
       WRITE (6,117)
       WRITE(6,104) THETAD,PH,DCNR2,DCNI2
C      COMPUTE END POINTS FOR THETA.
       CALL CALENP
       DO 140 I = 1,NSECT
       EPDEG(I) = RTD*EPPS(I)
  140  CONTINUE
       WRITE(6,148) (EPDEG(I),I=1,NSECT)
       RETURN
  190  WRITE (6,201)
       STOP
   80  FORMAT(5I12)
   88  FORMAT(1H144X,60H           CASES     MATRIX RANK        SECTIONS
      1 BODY SHAPE)
   92  FORMAT(1H044X,4I15)
   96  FORMAT(5E12.5,I12)
  117  FORMAT(1H025X,79HVARIOUS  PARAMETERS          THETAD              PH
      1           DCNR2           DCNI2)
  100  FORMAT(1H029X,75HBODY PARAMETERS            K(A)           AOVRB
      1          WN     DIELECTRIC1)
  104  FORMAT(1H044X,5F15.3)
  120  FORMAT(24HO    INTEGRATIONS/SECTION8I12,/(1H023X,8I12))
  148  FORMAT(24HO               END POINTS8F12.4,/(1H023X,8F12.4))
  201  FORMAT(1HO,23H***** END OF DATA *****)
       END
       SUBROUTINE GENLGP
C      A ROUTINE TO GENERATE LEGENDRE POLYNOMIALS.
C      THE INDEX ON THE FUNCTION IS INCREMENTED BY ONE.
       COMMON /MTXCOM/ NRANK,NRANKI
       COMMON DTR,RTD,CPI
       COMMON /ENCCOM/ PNMLLG(41)
       COMMON /CMVCOM/ NM,KMV,CMI(40),CMV,CM2,TWM,PRODM
       COMMON /THTCOM/ THETA,SINTH,COSTH,CDH(6),EPPS(6),NSECT,NDPS(6)
       DTWM = TWM+1.0
       IF(THETA)16,4,16
    4  IF(KMV-1)6,12,6
    6  DO 8 ILG = 1,NRANKI
       PNMLLG(ILG) = 0.0
    8  CONTINUE
       GO TO 88
   12  PNMLLG(1) = 0.0
       PNMLLG(2) = 1.0
       PLA = 1.0
       GO TO 48
```

```
   16 IF(KMV)20,20,40
C     THE SPECIAL CASE WHEN M = 0.
   20 PLA = 1.0/SINTH
      PLB = COSTH*PLA
      PNMLLG(1) = PLA
      PNMLLG(2) = PLB
      IBEG = 3
      GO TO 60
C     GENERAL CASE FOR M NOT EQUAL TO 0.
   40 DO 44 ILG = 1,KMV
      PNMLLG(ILG) = 0.0
   44 CONTINUE
      PLA = PRODM*SINTH**(KMV-1)
      PNMLLG(KMV+1) = PLA
   48 PLB = DTWM*COSTH*PLA
      PNMLLG(KMV+2) = PLB
      IBEG = KMV+3
C     DO RECURSION FORMULA FOR ALL REMAINING LEGENDRE POLYNOMIALS.
   60 CNMUL = IBEG+IBEG-3


      CNM = 2.0
      CNMM = DTWM
      DO 80 ILGR = IBEG,NRANKI
      PLC = (CNMUL*COSTH*PLB-CNMM*PLA)/CNM
      PNMLLG(ILGR) = PLC
      PLA = PLB
      PLB = PLC
      CNMUL = CNMUL+2.0
      CNM = CNM+1.0
      CNMM = CNMM+1.0
   80 CONTINUE
   88 RETURN
      END
      SUBROUTINE GENBKR
C     GENERATE BESSEL FUNCTIONS FOR COMPLEX ARGUMENTS.
C     THE INDEX ON THE FUNCTION IS INCREMENTED BY ONE.
      COMPLEX CKPR,RJ(410),A,PX,BSLCMP,CNEUM,CKR2
      COMMON DTR,RTD,CPI
      COMMON /MTXCOM/ NRANK,NRANKI
      COMMON /ENCCOM/ PNMLLG(41),BSLCMP(41),CNEUM(41),BSLKPR(41),BSLKPI
     1(41)
      COMMON /BDYCOM/ DCNR,DCNI,CKPRR,CKPRI,CKR,DCKR,CONK,AOVRB,WN,IB
      COMMON /THTCOM/ THETA,SINTH,COSTH,CDH(6),EPPS(6),NSECT,NDPS(6)
      DIMENSION KM(410),L(41)
      CKPR = CMPLX(CKPRR,CKPRI)
      PM = CABS(CKPR)
      DO 45 NBES = 1,5
      NVAL = 2*NRANKI*NBES
C
C     GENERATE BESSEL FUNCTIONS.
C
      RJ(NVAL+1) = (0.0,0.0)
      RJ(NVAL) = (1.0,0.0)
```

```
      IF(RM.GT.2.0) RJ(NVAL) = (1.0E-10,0.0)
      IF(RM.GT.10.0) RJ(NVAL) = (1.0E-20,0.0)
      IF(RM.GT.25.0) RJ(NVAL) = (1.0E-30,0.0)
      IE=NVAL+2
      A = CSIN(CKPR)/CKPR
      K = 0
      DO 10 I=2,NVAL
      IJ=IE-I
      RJ(IJ-1) = RJ(IJ)*FLOAT(2*IJ-1)/CKPR-RJ(IJ+1)
      IF(CABS(RJ(IJ-1)).GT.1.0E10) GO TO 8
      GO TO 9
    8 K = K+1
      RJ(IJ-1) = RJ(IJ-1)*1.0E-10
      RJ(IJ) = RJ(IJ)*1.0E-10
      KM(IJ) = K
    9 KM(IJ-1) = K
   10 CONTINUE
      PX = A/RJ(1)
      L(1) = 0
      DO 15 J = 2,NRANKI
      L(J) = L(J-1)
      IF(KM(J).NE.KM(J-1)) L(J) = L(J-1)+1
   15 CONTINUE
      DO 20 I=1,NRANKI
      BSLCMP(I) = RJ(I)*PX*10.0**(-L(I)*10)
      BSLKPR(I) = REAL(BSLCMP(I))
      BSLKPI(I) = AIMAG(BSLCMP(I))
   20 CONTINUE
C
C     GENERATE NEUMANN FUNCTIONS FOR TEST.
C


      CNEUM(1) = -CCOS(CKPR)/CKPR
      CNEUM(2) = CNEUM(1)/CKPR-A
      DO 30 I=3,NRANKI
      CNEUM(I) = CNEUM(I-1)*FLOAT(2*I-3)/CKPR-CNEUM(I-2)
   30 CONTINUE
C
C     PERFORM TWO TESTS ON BESSEL AND NEUMANN FUNCTIONS.  FIRST TEST IS
C     MOST ACCURATE FOR LARGE ARGUMENTS AND THE SECOND IS MOST ACCURATE
C     FOR SMALLER ARGUMENTS.  IF EITHER TEST IS PASSED, FUNCTIONS ARE GOOD.
C
C     FOR LARGE ARGUMENTS ABS(BESSEL) SHOULD EQUAL ABS(NEUMANN).
      C = 1.0E-05
      QUART = CABS(BSLCMP(1))/CABS(CNEUM(1))-1.0
      QUANT = CABS(BSLCMP(NRANKI))/CABS(CNEUM(NRANKI))-1.0
      IF((ABS(QUART).GT.C).OR.(ABS(QUANT).GT.C)) GO TO 32
      RETURN
C     PERFORM WRONSKIAN TEST IF LARGE ARGUMENT TEST FAILS.
   32 CKR2 = CKPR**2
C     BESSEL TEST
      QUANRT = CABS(CKR2*(BSLCMP(2)*CNEUM(1)-BSLCMP(1)*CNEUM(2))-1.0)
C     NEUMANN TEST
```

```
      QUANNT = CABS(CKR2*(BSLCMP(NRANKI)*CNEUM(NRANK)-BSLCMP(NRANK)*CNEU
     1M(NRANKI))-1.0)
      IF((QUANBT.GT.C).OR.(QUANNT.GT.C)) GO TO 45
      RETURN
   45 CONTINUE
   46 THTPRT = RTD*THETA
   60 RETURN
      END
      SUBROUTINE PRCSSM
C     A ROUTINE TO SOLVE THE EQUATION T = (A-INVERSE)*B  ( ALL MATRICES
C     ARE TRANSPOSED) USING GAUSS-JORDAN ELIMINATION.
      COMPLEX A,B,AIJMAX,ARAT,TMAT(80,80)
      COMMON /MTXCOM/ NR,NRI,A(80,80),B(80,80)
      COMMON /OUTCOM/ IOUT
      EQUIVALENCE (L,FL),(K,FK),(B(1,1),TMAT(1,1))
      N = 2*NR
C     START REDUCTION OF THE A MATRIX.
      DO 80 I = 1,N
C     SEARCH FOR THE MAXIMUM ELEMENT IN THE ITH ROW OF THE A-MATRIX.
      AIJMAX = A(I,1)
      JMAX = 1
      DO 10 J = 2,N
      IF(CABS(A(I,J)).LE.CABS(AIJMAX)) GO TO 10
      AIJMAX = A(I,J)
      JMAX = J
   10 CONTINUE
C     IF AIJMAX IS ZERO ( AS IT WILL BE FOR ANY ROW (OR COLUMN) WHERE THE
C     INDEX M IS .GT. THE INDEX N, I.E., THE LEGENDRE FUNCTIONS FORCE THOSE
C     MATRIX ELEMENTS TO ZERO),THEN THE MATRIX IS SINGULAR SO SOLVE THE
C     REDUCED MATRIX (ORDER = 2*(NRANK-M)).
      IF(CABS(AIJMAX).GT.0.0) GO TO 20
      JMAX = I
      GO TO 75
C     NORMALIZE THE ITH ROW BY AIJMAX (JMAX ELEMENT OF THE ITH ROW).
   20 DO 30 J = 1,N
      A(I,J) = A(I,J)/AIJMAX
C     NORMALIZE THE ITH ROW OF B.
      B(I,J) = B(I,J)/AIJMAX
   30 CONTINUE
C     USE ROW TRANSFORMATIONS TO GET ZEROS ABOVE AND BELOW THE JMAX
C     ELEMENT OF THE ITH ROW OF A.  APPLY SAME ROW TRANSFORMATIONS
C     TO THE B MATRIX.
      DO 70 K = 1,N


      IF(K.EQ.I) GO TO 70
      ARAT = -A(K,JMAX)
      DO 50 J = 1,N
      IF(CABS(A(I,J)).LE.0.0) GO TO 50
      A(K,J) = ARAT*A(I,J)+A(K,J)
   50 CONTINUE
      A(K,JMAX) = 0.0
      DO 60 J=1,N
      IF(CABS(B(I,J)).LE.0.0) GO TO 60
      B(K,J) = ARAT*B(I,J)+B(K,J)
```

```
   60 CONTINUE
   70 CONTINUE
C     STORE ROW COUNTER (I) IN TOP ELEMENT OF JMAX COLUMN.  THUS,
C     THE TOP ROW OF A WILL CONTAIN THE LOCATION OF THE PIVOT
C     (UNITY) ELEMENT OF EACH COLUMN (AFTER REDUCTION).
   75 L = I
C     STORE THE INTEGER I IN THE TOP ROW OF A.
      A(1,JMAX)   = FL
   80 CONTINUE
C     THE REDUCTION OF A IS COMPLETE.  PERFORM ROW INTERCHANGES
C     AS INDICATED IN THE FIRST ROW OF A.
      DO 120 I = 1,N
      K=I
C     PUT THE INTEGER VALUE IN A INTO K.
   90 FK = A(1,K)
      IF(K-I) 90,120,100
C     IF K(1,I) IS LESS THAN I, THEN THAT ROW HAS ALREADY BEEN
C     INVOLVED IN AN INTERCHANGE, AND WE USE K(1,K) UNTIL WE GET
C     A VALUE OF K GREATER THAN I (CORRESPONDING TO A ROW STORED
C     BELOW THE ITH ROW).
  100 DO 171 J=1,N
      APAT = B(I,J)
      B(I,J) = B(K,J)
      B(K,J) = APAT
  171 CONTINUE
  120 CONTINUE
C     THE TRANSPOSED T MATRIX IS STORED IN B.  TRANSPOSE TO GET THE T
C     MATRIX AND STORE IN A.
      DO 140 I = 1,N
      DO 130 J = 1,N
      A(I,J) = B(J,I)
  130 CONTINUE
  140 CONTINUE
C     TRANSFER THE T MATRIX FROM A INTO TMAT.
      DO 160 I = 1,N
      DO 150 J = 1,N
      TMAT(I,J) = A(I,J)
  150 CONTINUE
  160 CONTINUE
      CALL ADDPRC
      RETURN
      END
      SUBROUTINE ADDPRC
C     A ROUTINE TO OBTAIN THE SCATTERED FIELD COEFFICIENTS AND CALCULATE
C     THE TOTAL NEAR FIELD IN THE AZIMUTHAL PLANE PHI = CONSTANT.
      COMPLEX A,TMAT,AD1(80),AD2(80),ENGANS(361,2),H1(41),H2(41),BJ1(41)
     1,BJ2(41),CI,THC,PHC,RC,CKPR,DCN,DCN2,RHO,RHOP,HANK(41),ACANS,
     2ACANSP,BSSLSP,CNEUMN,PCOMP(361),S1,S2,HANKP(41),BSSLPP(41),
     3CNEUMP(41),AD1X(80),AD1Z(80),AD2Y(80),SI,PX,PY,PZ,FG1(80),FG2(80),
     4W,ETHETA,EPHI,ER,ETH(361),EPH(361),ERC(361)
      COMMON DTR,RTD,CPI
      COMMON /MTXCOM/ NRANK,NRANKI,A(80,80),TMAT(80,80),CMXNRM(80)
      COMMON /ENCCOM/ PNMLLG(41),BSSLSP(41),CNEUMN(41),BSLKPR(41),
     1BSLKPI(41)
```

```
      COMMON /BDYCOM/ DCNR,DCNI,CKPRR,CKPRI,CKR,DCKR,CONK,AOVRB,WN,IB
      COMMON /CMVCOM/ NM,KMV,CMI(40),CMV,CM2,TWM,PRODM
      COMMON /THTCOM/ THETA,SINTH,COSTH,COH(6),EPPS(6),NSECT,NDPS(6)
     1,THETAD,PH,KSECT
      COMMON/UVCCOM/ACANS(361,2),ACANSR(361),DLTANG,DCNR2,DCNI2,NUANG
      COMMON /OUTCOM/ IOUT
      DIMENSION ZXOLD(361),ZYOLD(361),ZROLD(361)
      LOGICAL TEST
      DATA TEST/.TRUE./
      NR2 = 2*NRANK
C
C     GENERATE THE INCIDENT DIPOLE COEFFICIENTS AD1 AND AD2.
C
      CI = (0.0,1.0)
      DCN = CMPLX(DCNR,DCNI)
      DCN2 = CMPLX(DCNR2,DCNI2)
      W = WN*CSQRT(DCN2)
      SI = CI*(W**3)/(CPI*DCN2*8.854E-12)
C     RHOP IS THE RADIAL COORDINATE OF THE DIPOLE TIMES THE WAVE NUMBER.
      RHOP = CONK*1.05*CSQRT(DCN2)
      CKPRR = REAL(RHOP)
      CKPRI = AIMAG(RHOP)
      CALL GENBKR
      DO 36 I=1,NRANKI
      BSSLPP(I) = BSSLSP(I)
      CNEUMP(I) = CNEUMN(I)
      HANKP(I) = BSSLPP(I) + CI*CNEUMP(I)
   36 CONTINUE
      RHO = CONK*1.1*CSQRT(DCN2)
      CKPRR = REAL(RHO)
      CKPRI = AIMAG(RHO)
      CALL GENBKR
      DO 37 I=1,NRANKI
      HANK(I) = BSSLSP(I) +CI*CNEUMN(I)
   37 CONTINUE
      CN = 0.0
C     GENERATE LEGENDRE FUNCTIONS FOR DIPOLE ANGULAR COORDINATE THETAD.
      THETA = DTR*THETAD
      CALL TRIG(THETAD,SINTH,COSTH)
      CALL GENLGP
      DO 35 N=1,NRANK
      NP = N+NRANK
      CN = CN+1.0
      N1 = N+1
      P1 = CN*COSTH*PNMLLG(N1)-(CN+CMV)*PNMLLG(N)
      P2 = CMV*PNMLLG(N1)
      CKPR = RHOP
      BJ1(N) = N*N1*BSSLPP(N1)/CKPR
      BJ2(N) = BSSLPP(N) - (N/CKPR)*BSSLPP(N1)
      PX = 1.0
      PY = 0.0
      PZ = 0.0
      AD1X(N) = COSTH*P2*BSSLPP(N1)
      AD1Z(N) = -BSSLPP(N1)*SINTH*P2
```

```
      AD1X(NP) = BJ1(N)*PNMLLG(N1)*(SINTH**2) + BJ2(N)*COSTH*P1
      AD1Z(NP)=BJ1(N)*SINTH*COSTH*PNMLLG(N1)-BJ2(N)*SINTH*P1
      AD2Y(N) = -P1*BSSLPP(N1)
      AD2Y(NP) = -P2*BJ2(N)
      AD1(N) = (PX*AD1X(N) + PZ*AD1Z(N))*SI
      AD1(NP) = (PX*AD1X(NP) + PZ*AD1Z(NP))*SI
      AD2(N) = PY*AD2Y(N)*SI
      AD2(NP) = PY*AD2Y(NP)*SI
   35 CONTINUE
C
C
C     THE SCATTERED FIELD COEFFICIENTS = THE TRANSITION MATRIX TIMES THE
C     INCIDENT FIELD COEFFICIENTS.
C
      DO 45 I = 1,NR2
      S1 = 0.0
      S2 = 0.0
      DO 40 J = 1,NR2
      S1 = S1 + TMAT(I,J)*AD1(J)
      S2 = S2 + TMAT(I,J)*AD2(J)
   40 CONTINUE
      FG1(I) = S1
      FG2(I) = S2
   45 CONTINUE
C
C     EVALUATE THE SCATTERED FIELD AT EACH SCATTERING ANGLE.
C
      DO 170 IU = 1,NUANG
C     GENERATE THE LEGENDRE MULTIPLIERS.
      THETT = DLTANG*(IU - 1)
      IF (THETT.LE.181.0) GO TO 62
      PHP = PH + 180.0
      THET = 360.0 - THETT
      THETA = DTR*THET
      SINTH = SIN(THETA)
      COSTH = COS(THETA)
      CALL GENLGP
      PHI = CMV*PHP
      GO TO 61
   62 IF(THETT) 95,85,95
   85 COSTH = 1.0
      KODE = 0
   91 SINTH = 0.0
      THETA = 0.0
      GO TO 119
   95 IF(THETT-180.0) 105,101,105
  101 COSTH = -1.0
      KODE = 180
      GO TO 91
  105 THETA = DTR*THETT
      SINTH =  SIN(THETA)
      COSTH =  COS(THETA)
  119 CALL GENLGP
      PHI = CMV*PH
```

```
   61 CALL TRIG(PHI,SINPHI,COSPHI)
      ENGANS(IU,1) = 0.0
      ENGANS(IU,2) = 0.0
      RCOMP(IU) = 0.0
      CN = 0.0
      DO 160 N = 1,NRANK
      NP = N+NRANK
      N1 = N+1
      CN = CN+1.0
      P1 = CN*COSTH*PNMLLG(N1)-(CN+CMV)*PNMLLG(N)
      P2 = CMV*PNMLLG(N1)
      AA=SINPHI*P1
      BB=COSPHI*P1
      CC=SINPHI*P2
      DD=COSPHI*P2
      EE = PNMLLG(N1)*SINTH*COSPHI
      FF = PNMLLG(N1)*SINTH*SINPHI
      IF(KMV.NE.0) GO TO  48
      SGN = 1.0
      IF(THETA) 48,44,48
   44 IF(KODE.EQ.0) GO TO 46


      EGN = (-1.0)**N
   46 EE = COSPHI*SGN
      FF = SINPHI*SGN
   48 CONTINUE
C
C     CALCULATE THE THETA COMPONENT OF THE SCATTERED FIELD.
C
      CKPR = RHO
      H1(N) = N*N1*HANK(N1)/CKPR
      H2(N) = HANK(N) - (N/CKPR)*HANK(N1)
      ETHETA=(DD*EG1(N)-CC*EG2(N))*HANK(N1)+(BB*EG1(NP)-AA*EG2(NP))*H2(N
     1)
      ENGANS(IU,1) = ENGANS(IU,1) + ETHETA/CMXNRM(N)
C
C     CALCULATE THE PHI COMPONENT OF THE SCATTERED FIELD.
C
      EPHI=-(BB*EG2(N)+AA*EG1(N))*HANK(N1)-(CC*EG1(NP)+DD*EG2(NP))*H2(N)
      ENGANS(IU,2) = ENGANS(IU,2) + EPHI/CMXNRM(N)
C
C     CALCULATE THE R COMPONENT OF THE SCATTERED FIELD.
C
      ER = (EE*EG1(NP)-FF*EG2(NP))*H1(N)
      RCOMP(IU) = RCOMP(IU) + ER/CMXNRM(N)
  160 CONTINUE
  170 CONTINUE
C     ACCUMULATE THE RESULTS FOR EACH M VALUE.
      DO 172 IUP = 1,NUANG
      ACANS(IUP,1) = ACANS(IUP,1) + ENGANS(IUP,1)
      ACANS(IUP,2) = ACANS(IUP,2) + ENGANS(IUP,2)
      ACANSR(IUP) = ACANSR(IUP)+RCOMP(IUP)
  172 CONTINUE
```

```
C     PRINT THE FIELD COMPONENTS AND THEIR MODULI SQUARED.
      WRITE(6,175) KMV
  175 FORMAT(1H1,35X,35H********** ACCUMULATED SUMS FOR M =,I3,11H *****
     1*****/1HO,40X,17HTOTAL NEAR FIELDS/1HO,1X,5HANGLE,12X,15HTHETA COM
     2PONENT,14X,13HPHI COMPONENT,16X,11HR-COMPONENT,22X,5HTOTAL//)
      NCONV = 0
      MCONV = 0
      LCONV = 0
      SCANG = 0.0
      CALL DIPOLE(ETH,EPH,ERC)
C     ADD DIPOLE FIELDS ETH,EPH,ERC TO OBTAIN TOTAL FIELDS.
      DO 190 JUP = 1,NUANG
      THC = ACANS(JUP,1) + ETH(JUP)
      PHC = ACANS(JUP,2) + EPH(JUP)
      RC = ACANSR(JUP) + ERC(JUP)
C     THC = THETA COMPONENT OF TOTAL FIELD.
C     PHC = PHI COMPONENT OF TOTAL FIELD.
C     RC = R COMPONENT OF TOTAL FIELD.
      X = CABS(THC)**2
      Y = CABS(PHC)**2
      R = CABS(RC)**2
      ESQ = X+Y+R
      WRITE (6,181) SCANG,X,Y,R,ESQ
  181 FORMAT (1H ,F6.2,4(12X,E15.6))
C     TEST FOR CONVERGENCE AT EACH ANGLE.
      IF(TEST) GO TO 184
      IF( ABS(X - ZXOLD(JUP)).LE.(X*1.0E-03)) NCONV = NCONV + 1
      IF( ABS(Y - ZYOLD(JUP)).LE.(Y*1.0E-03)) MCONV = MCONV + 1
      IF( ABS(R - ZROLD(JUP)).LE.(R*1.0E-03)) LCONV = LCONV + 1
  184 ZXOLD(JUP) = X
      ZYOLD(JUP) = Y
      ZROLD(JUP) = R
      SCANG = SCANG+DLTANG


  190 CONTINUE
C     TEST FOR COMPLETE CONVERGENCE OF SOLUTION.
  198 IF(NCONV.EQ.NUANG.AND.MCONV.EQ.NUANG.AND.LCONV.EQ.NUANG) GO TO 194
      TEST = .FALSE.
C
      RETURN
  194 WRITE(6,200)
  200 FORMAT(1HO,30H*** SOLUTION HAS CONVERGED ***)
   14 CONTINUE
      STOP
      END
      SUBROUTINE TRIG(A,SINN,COSN)
      COMMON DTR,RTD,CPI
      SINN = SIN(DTR*A)
      COSN = COS(DTR*A)
      IF(A-180.0) 5,10,15
    5 IF(A+180.0) 15,10,15
   10 SINN = 0.0
   15 IF(A-90.0) 20,25,30
   20 IF(A+90.0) 30,25,30
   25 COSN = 0.0
   30 RETURN
      END
```

```
      SUBROUTINE CALENP
C     CALCULATE THE ANGULAR ENDPOINTS FOR EACH SECTION OF THE BODY.
      COMMON DTR,RTD,CPI
      COMMON /BDYCOM/ DCNR,DCNI,CKPRR,CKPRI,CKR,DCKR,CONK,AOVRB,WN,IB
      COMMON /THTCOM/ THETA,SINTH,COSTH,CDH(6),EPPS(6),NSECT,NDPS(6)
      EPPS(1)=CPI/2.0
      CDH(1) = EPPS(1)/NDPS(1)
      RETURN
      END
      SUBROUTINE GENKR
C     CALCULATE CKR AND DCKR AS A FUNCTION OF THETA FOR A PROLATE SPHEROID.
      COMMON /BDYCOM/ DCNR,DCNI,CKPRR,CKPRI,CKR,DCKR,CONK,AOVRB,WN,IB
      COMMON /THTCOM/ THETA,SINTH,COSTH,CDH(6),EPPS(6),NSECT,NDPS(6)
      QR = 1.0/SQRT(COSTH**2+(AOVRB*SINTH)**2)
      CKR = CONK*QR
      DCKR = -CONK*COSTH*SINTH*(AOVRB**2-1.0)*QR**3
      RETURN
      END
      SUBROUTINE DIPOLE(ETH,EPH,ERC)
C     A SUBROUTINE TO CALCULATE THE FIELD DUE TO A DIPOLE AT COORDINATE
C     (RD,THD,0.0) AND COMPONENTS (PX,PY,PZ)
C     ETH = THETA COMPONENT OF ELECTRIC FIELD AT OBSERVER COORDINATE (RO
C     ,SCANG,PH/PHP).
C     EPH = PHI COMPONENT
C     ERC = R-COMPONENT
C     W = WAVE NUMBER IN OBSERVERS MEDIUM.
C     D = DISTANCE BETWEEN DIPOLE AND OBSERVER.
      COMPLEX U,V,W,CI,PX,PY,PZ,ETH(361),EPH(361),ERC(361),DCN2,FAC,CE,
     1ACANS,ACANSP
      COMMON DTR,RTD,CPI
      COMMON /BDYCOM/ DCNR,DCNI,CKPRR,CKPRI,CKR,DCKR,CONK,AOVRB,WN,IB
      COMMON /THTCOM/ THETA,SINTH,COSTH,CDH(6),EPPS(6),NSECT,NDPS(6)
     1,THETAD,PH,KSECT
      COMMON/UVCCOM/ACANS(361,2),ACANSP(361),DLTANG,DCNR2,DCNI2,NUANG
      THD = THETAD*DTR
      CI = (0.0,1.0)
      PX = 1.0
      PY = 0.0
      PZ = 0.0
      RD = 1.05*CONK/WN
      RO = 1.1*CONK/WN


      DO 11 I = 1,NUANG
      SCANG = (I-1)*DLTANG
      IF (SCANG.LE.181.0) GO TO 8
      SCAN = 360.0-SCANG
      THETA = SCAN*DTR
      SINTH = SIN(THETA)
      COSTH = COS(THETA)
      PHP = 180.0+PH
      PHD = PHP*DTR
      GO TO 9
```

```
  8 THETA = SCANG*DTR
    SINTH = SIN(THETA)
    COSTH = COS(THETA)
    PHD = PH*DTR
  9 RX = RD*SINTH*COS(PHD)-RD*SIN(THD)
    RY = RD*SINTH*SIN(PHD)
    RZ = RD*COSTH - RD*COS(THD)
    D = SQRT(RX**2+RY**2+RZ**2)
    R1=RX*SINTH*COS(PHD)+RY*SINTH*SIN(PHD)+RZ*COSTH
    R2=RX*COSTH*COS(PHD)+RY*COSTH*SIN(PHD)-RZ*SINTH
    R3=RY*COS(PHD)-RX*SIN(PHD)
    DCN2 = CMPLX(DCNR2,DCNI2)
    W = WN*CSQRT(DCN2)
    U = (W**2)/D + CI*W/D**2 - 1/D**3
    V = 3.0*(1/D**5 - CI*W/D**4) - (W**2)/D**3
    FAC = 1/(4.0*CPI*DCN2*8.854E-12)
    CE = CEXP(CI*W*D)
    ETH(I) = FAC*(PY*(U*COSTH*COS(PHD)+V*RX*R2)+PY*(U*COSTH*SIN(PHD)
   1+V*RY*R2)+PZ*(V*RZ*R2-U*SINTH))*CE
    EPH(I) = FAC*(PX*(V*RX*R3-U*SIN(PHD))+PY*(U*COS(PHD)+V*RY*R3)+PZ*
   1V*RZ*R3)*CE
    ERC(I) = FAC*(PX*(U*SINTH*COS(PHD)+V*RX*R1)+PY*(U*SINTH*SIN(PHD)+
   1V*RY*R1)+PZ*(U*COSTH+V*RZ*R1))*CE
 11 CONTINUE
    RETURN
    END
```

NBS-114A (REV. 2-8C)

| U.S. DEPT. OF COMM. BIBLIOGRAPHIC DATA SHEET (See instructions) | 1. PUBLICATION OR REPORT NO. NBSIR 81-1653 | 2. Performing Organ. Report No. | 3. Publication Date November 1981 |
|---|---|---|---|

4. TITLE AND SUBTITLE

Modelling of Oil Shale Retorts for Electromagnetic Sensing Techniques

5. AUTHOR(S)

H. Chew *

6. PERFORMING ORGANIZATION (If joint or other than NBS, see instructions)

NATIONAL BUREAU OF STANDARDS
DEPARTMENT OF COMMERCE
WASHINGTON, D.C. 20234

7. Contract/Grant No.
PR No. 20-802C10417.000

8. Type of Report & Period Covered
Final Report

9. SPONSORING ORGANIZATION NAME AND COMPLETE ADDRESS (Street, City, State, ZIP)

U.S. Department of Energy
Laramie Energy Technology Center
Laramie, Wyoming 82071

10. SUPPLEMENTARY NOTES

*On sabbatical leave (1980-1981) from Department of Physics, Clarkson College, Potsdam, NY 13676.

☐ Document describes a computer program; SF-185, FIPS Software Summary, is attached.

11. ABSTRACT (A 200-word or less factual summary of most significant information. If document includes a significant bibliography or literature survey, mention it here)

We report here some work on the modelling of oil shale retorts for electromagnetic sensing techniques. The aim is to obtain useful information about the contents of the retort (e.g., rubble size, void ratio, etc.) by means of electromagnetic probes. In this work, the retort is modelled by a spheroid with an average dielectric constant which depends on the void ratio. The near field due to a radiating dipole source in the vicinity of a spheroidal retort is computed using the Extended Boundary Condition Method due to Waterman, Barber, and Yeh. Numerical results are given at 4 MHz for a retort with major axis 45.7 (150 ft ), minor axis 25.1 m (82.5 ft ), bulk dielectric constant 8.8 + 3.7j, and various void ratios. The results indicate feasibility of determining the void ratio by remote electromagnetic measurements. It is also believed that this work may be of interest beyond the immediate context of oil shale retort modelling.

12. KEY WORDS (Six to twelve entries; alphabetical order; capitalize only proper names; and separate key words by semicolons)

Oil shale retorts; remote sensing; scattering

13. AVAILABILITY

☒ Unlimited
☐ For Official Distribution. Do Not Release to NTIS
☐ Order From Superintendent of Documents, U.S. Government Printing Office, Washington, D.C. 20402.
☒ Order From National Technical Information Service (NTIS), Springfield, VA. 22161

14. NO. OF PRINTED PAGES
48

15. Price
$6.50

USCOMM-DC 6043-P80

☆ U.S. GOVERNMENT PRINTING OFFICE: 1981—576-001/1214 Region No. 8